Development of a Model to Predict the Adsorption of Lead from Solution on a Natural Streambed Sediment

United States
Geological
Survey
Water-Supply
Paper 2187

Development of a Model to Predict the Adsorption of Lead from Solution on a Natural Streambed Sediment

By D. W. BROWN and J. D. HEM

U.S. GEOLOGICAL SURVEY WATER-SUPPLY PAPER 2187

UNITED STATES DEPARTMENT OF THE INTERIOR
WILLIAM P. CLARK, Secretary

GEOLOGICAL SURVEY
Dallas L. Peck, Director

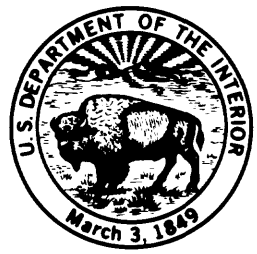

UNITED STATES GOVERNMENT PRINTING OFFICE, WASHINGTON : 1984

For sale by the Superintendent of Documents
U. S. Government Printing Office
Washington, DC 20402

Library of Congress Cataloging in Publication Data

Brown, David Wayne, 1949–
Development of a model to predict the adsorption of lead from solution on a natural streambed sediment.

(Geological Survey water-supply paper, 2187)
Bibliography: p.
Supt. of Docs. no.: I 19.13:
1. Adsorption—Mathematical models. 2. Lead compounds—Mathematical models. 3. Water chemistry—Mathematical models. 4. Silt—California—Colma Creek.
I. Hem, John David, 1916–. II. Title. III. Series.
QD547.B76 628.1'6836 81–607984
AACR2

CONTENTS

FIGURES

FIGURES

TABLES

Development of a Model to Predict the Adsorption of Lead from Solution on a Natural Streambed Sediment

By D. W. Brown *and* J. D. Hem

Abstract

Adsorption of solutes by solid mineral surfaces commonly influences the dissolved ionic composition of natural waters. A model based on electrical double-layer theory has been developed which appears to be capable of characterizing the surface chemical behavior of a natural fine-grained sediment containing mostly quartz and feldspar. This variable surface charge–variable surface potential (VSC–VSP) model differs from others in being capable of evaluating more closely the effect of total metal ion activity on the pH-dependent change in electrical potential at the solid surface. The model was tested using 10^{-4} molar solutions of lead and a silt-size fraction of sediment from the bed of Colma Creek, a small stream in urban northern San Mateo County, California. The average deviation of measured percent adsorption and values calculated from the model was 6.6 adsorption percent from pH 2.0 to pH 7.0

INTRODUCTION

The purpose of the study described in this paper is to develop a theoretically based semiempirical model for the behavior of certain natural silicate mineral surfaces in aqueous solutions toward dissolved metal ions. A practical application of the model is then described in which it is used to predict successfully the degree of adsorption of dissolved lead ions over the pH range of 2.0–9.0. The substrate used in this application is a fine-grained fraction of a natural streambed sediment, consisting predominantly of weathered quartz and feldspar.

In order to place the topic of surface-chemical effects in proper perspective in the field of natural water chemistry, a brief description of the major principles and their effects is appropriate.

CHEMICAL PROCESSES AFFECTING LEAD SOLUBILITY

The extensive use of lead antiknock additives in gasoline has made lead perhaps the most widely distributed toxic heavy metal in the urban environment, and this use has greatly increased its availability for solution in natural waters. It is important for this reason to study chemical processes in surface and ground water that limit its solubility, and evaluate their effectiveness.

A model for predicting the concentrations of lead in surface or ground water must accurately reflect the actual physical and chemical processes that affect the distribution of lead between the solid and dissolved aqueous phases. In a natural water system, the chemical processes that can strongly influence the concentrations of lead may be divided into the categories of complex formation, precipitation, and adsorption or cation exchange (Stumm and Morgan, 1970).

ADSORPTION UPON SOLID SURFACES

Adsorption is generally defined as the process by which one substance is accumulated on the surface of another. In the narrower context of processes in heterogeneous aqueous systems, it is the process by which solute ions or molecules are attracted to and retained by solid surfaces exposed to the solution. Solvent molecules also may be adsorbed. This definition says nothing specific about the mechanisms involved, but to most scientific users of the term "adsorption" implies a reversible process in which the adsorbing surface undergoes no permanent chemical alteration.

The broader term "absorption" implies the taking up of a substance, or energy form, by another substance, without implications as to either processes or physical location.

Some of the processes by which solid surfaces take up solutes entail considerable alteration of the surface. For example, adsorbed species may interact with surface ions of the solid or with other adsorbed material and produce an altered surface layer or a layer of new precipitate. Some solutes, notably large organic molecules, may form an adsorbed layer with properties very different from those of the original surface. These processes may also be reversible although generally not as readily as those involving only electrostatic forces or interfacial energy gradients. Methods for studying the systems are not always capable of distinguishing among these processes and some writers have preferred to use the term "sorption" to lump together all processes by which solutes interact with and are taken up by solid surfaces.

Adsorption is used here to indicate processes by which solute ions are held at solid-liquid interfaces by electrostatic and specific chemical interactions. Oxide

and silicate surfaces generally consist of close-packed oxygen lattices, and because of their anionic nature there is a residual negative electrostatic charge over the surface. More intense sites of negative charge may occur where there are lattice imperfections, or where positive charge deficiencies occur near cation sites, as where an Al^{+3} ion might be substituted for a Si^{+4}. Where there are broken chemical bonds, as where the continuous sheet lattice of layered silicates is terminated at crystal edges and corners, there will also be highly charged sites, with either negative or positive sign.

Near the more highly charged sites, cations from solutions may become attached through interactions that involve chemical bonding. This type of adsorption has commonly been referred to as cation exchange, but it is not usually possible to distinguish experimentally this kind of adsorption from other adsorption processes.

CHARACTERIZATION OF NATURAL MINERAL SURFACES

The total amount of mineral surface in contact with a specific volume of stored water in the soil or in a partly or fully saturated granular aquifer is large, and the capacity for adsorption associated with that volume of water may approach or even exceed the concentrations of major cations in solution. As water moves through the pores of enclosing solids, the effects of adsorption and ion-exchange processes can become even more marked, and the surface contacted by a liter of water in such a system can add up to many thousands of square meters during movement of the liter of water from a point of introduction to a point of withdrawal. Interaction and exchange between dissolved and adsorbed solutes can dominate other processes and maintain characteristic ratios of major cations, as in the natural softening effects that have been observed in many ground-water systems.

Although the soil-mineral surface area encountered by a liter of river water during its transport toward the sea is considerably smaller, the interchange of sediment particles with the streambed material and the generally slower movement of sediment compared to that of the water does commonly provide extensive opportunity for adsorption and exchange processes in river water as well. Also, almost all river water has had at least some prior history as ground water or soil moisture.

In a mixed electrolyte solution the cations can be expected to compete for adsorption or exchange sites, and some will be held more strongly than others. Cations present in small amounts in solution can be greatly depleted by adsorption effects during relatively short distances of water movement if these cations were not present initially in the adsorbed material.

To predict the behavior of introduced solutes in natural systems where surface chemical processes are occurring requires some knowledge both of the capacity of the surface for adsorption of the solutes that are present, and of the relative extent of adsorption for the different solutes. The latter may be difficult to quantify because all the interactions among the solutes and surfaces may be influenced by relative, as well as absolute, concentrations.

Models developed for quantifying surface chemical processes range in sophistication from simple isotherms and distribution coefficients to relatively elegant electrical double-layer models. A review of the potential applications of the latter to natural materials has recently been published by James and Parks (1982).

Two of the simpler conceptual models that have been used to quantify adsorption effects are the applications of adsorption isotherms and the law of mass action. These approaches are fundamentally similar.

An adsorption isotherm is a mathematical statement relating the concentration of an adsorbed solute species on an adsorbing surface to the concentration of the free species in the solution. At a single temperature and pressure, a relationship of the form:

$$\frac{X_i}{m} = K\, C_i^n \qquad (1)$$

will generally occur over at least a part of the concentration range. The term X is the quantity of the solute species i adsorbed, m is weight of adsorbing substrate, C_i is the concentration of the solute in solution, and K and n are constants. This relationship is known as the Freundlich isotherm. Because there obviously is an upper limit to the amount of solute that can be adsorbed by a finite amount of substrate, the values of K and n are not constant over wide concentration ranges. Constants similar in derivation to K are sometimes called partition or distribution coefficients.

The Langmuir isotherm was developed to include the concept of a finite adsorptive capacity for the substrate. One form of this isotherm is

$$\theta_i = \frac{KC_i}{1+KC_i}\,, \qquad (2)$$

where θ represents the fraction of available adsorbing capacity that is occupied by the adsorbed species i, C_i is the concentration or thermodynamic activity in somewhat more sophisticated models of the ions in solution and K is an equilibrium constant.

The law of mass action has been sucessfully used in some instances to describe the phenomena in terms of cation exchange. In a cation exchange reaction between two univalent ions A^+ and B^+, the reaction is written:

$$AX + B^+_{aq} \rightleftharpoons BX + A^+_{aq}\,, \qquad (3)$$

where A^+_{aq} and B^+_{aq} are aqueous ionic species and AX and BX are the respective adsorbed forms of these ions. The

equilibrium expression given by Truesdell and Christ (1968) is

$$K_{AB} = \frac{[A^+]\ N_{BX}\lambda_{BX}}{[B^+]\ N_{AX}\lambda_{AX}}\ , \qquad (4)$$

where $[A^+]$ and $[B^+]$ are ionic activities of the aqueous species, N_{AX} and N_{BX} are the mole fractions with respect to the total adsorbed species, and λ_{AX} and λ_{BX} are the applicable rational activity coefficents. Since concentration conversion factors will cancel out in such an expression involving exchange of equally charged ions, solution concentration units, such as moles per liter, may be used to describe N_{AX} and N_{BX}.

For systems where more than one adsorbing species may occur, one may write a Langmuir isotherm in the form:

$$\theta_i = \frac{K_i^{ads}[i^{+z}]}{1+\sum K_i^{ads}[i^{+z}]}\ , \qquad (5)$$

where θ_i is the fraction of surface to which the cation is adsorbed, K is an equilibrium constant, and $[i^{+z}]$ is the aqueous activity of the adsorbing ion i^{+z} with charge $+z$. This isotherm is derived by treating the available surface sites as analogous to dissolved species in mass action expressions. The sum of the individual θ_i values is equal to Θ which is the overall fraction of charged surface sites to which any and all cations are adsorbed. The equilibrium constant for an adsorbed ion may be expressed as

$$K_i^{ads} = \frac{\theta_i}{[i^{+z}]\ (1-\Theta)}\ . \qquad (6)$$

Simultaneous adsorption of two univalent ions A^+ and B^+ may be described by the relations:

$$K_{A^+}^{ads} = \frac{\theta_{A^+}}{[A^+]\ (1-\Theta)} \qquad (7)$$

and

$$K_{B^+}^{ads} = \frac{\theta_{B^+}}{[B^+]\ (1-\Theta)}\ . \qquad (8)$$

We may divide the second relation by the first to obtain the expression:

$$\frac{K_{B^+}^{ads}}{K_{A^+}^{ads}} = \frac{[A^+]\ \theta_{B^+}}{[B^+]\ \theta_{A^+}}\ , \qquad (9)$$

which is identical to a cation exchange expression for cations A^+ and B^+, when activity coefficients are ignored or assumed equal to unity.

The situation is more complex for cation-exchange equilibrium relationships between ions of unlike charge. Several theories of cation exchange equilibrium have been proposed, and their mass action equilibrium expressions reduce to the type of relation noted above for ions of the same charge, but not for ions of unlike charge. Taking, as an example, the calcium-sodium cation exchange equilibrium,

$$CaX_2 + 2Na^+ \leftrightharpoons Ca^{+2} + 2NaX, \qquad (10)$$

a simple mass-action approach would seem to dictate the relation

$$K = \frac{[Ca^{+2}]\ N^2_{NaX}\lambda^2_{NaX}}{[Na^+]^2\ N_{CaX_2}\lambda_{CaX_2}}\ . \qquad (11)$$

The definition of mole fraction N of the adsorbed phase has been the subject of some debate. Vanselow (1932) proposed a theory which utilizes the above expression, but with adsorbed mole fractions N_{CaX_2} and N_{NaX} described by

$$N_{CaX_2} = (CaX_2)\ /\ [(CaX_2)+(NaX)] \qquad (12)$$

and

$$N_{NaX} = (NaX)\ /\ [(CaX_2)+(NaX)]. \qquad (13)$$

Using what they called the "statistical" approach, Krishnamoorthy and Overstreet (1949) alternatively suggested using

$$N_{CaX_2} = (CaX_2)\ /\ [3/2(CaX_2)+(NaX)] \qquad (14)$$

and

$$N_{NaX} = (NaX)\ /\ [3/2(CaX_2)+(NaX)], \qquad (15)$$

where the concentrations of divalent or trivalent ions in the adsorbed phase were multiplied by 3/2 and 2, respectively, in the denominators, apparently corresponding to the average of the absolute valences of the exchanged ion and the site. In either case, Vanselow's (1932) and Krishnamoorthy and Overstreet's (1949) equilibrium expressions for this system were written, respectively, as

$$K = \frac{(NaX)^2[Ca^{+2}]}{(Na^+)^2(CaX_2)[CaX_2)+(NaX)]} \qquad (16)$$

and

$$K = \frac{(NaX)^2[Ca^{+2}]}{(Na^+)\ (CaX_2)[3/2(CaX_2)\ +\ (NaX)]}\ , \qquad (17)$$

ignoring any deviations from ideality by assuming any activity coefficients to be unity.

Another approach is to treat the univalent-divalent cation exchange between Ca^{+2} and Na^{+} as consisting of the reaction:

$$Ca_{0.5}\,X + Na^{+} = 0.5\,Ca^{+2} + NaX\ , \qquad (18)$$

so that the equilibrium expression would be

$$K = \frac{(NaX)[Ca^{+2}]^{0.5}}{(Ca_{0.5}X)\ [Na^{+}]}\ . \qquad (19)$$

In brief summary, past work on cation exchange equilibria has produced numerous forms of equilibrium expressions for exchange between cations of different charge. One problem in determining which theory is "correct" is that the results from different systems seem to verify different expressions. Another problem is that some expressions are often only very subtly different from one another in terms of the predicted result, and, when the magnitude of experimental error is considered, several expressions still remain as possible correct explanations.

THE ELECTRICAL DOUBLE-LAYER CONCEPT

The James-Healy Model and Langmuir Isotherms

The electrical double-layer concept postulates that the surface of a solid in an aqueous system accumulates an immobile monolayer of water molecules that are tightly bound to the surface, and that additional layers at greater distances from the surface constitute a transition zone in physical behavior until the influence of the solid surface is no longer detectible. Outside the immobile layer there is an accumulation of solute ions with electrical charges opposite that of the surface, in an amount sufficient to maintain electrical neutrality. There may be some interactions strong enough to bring solute ions into direct contact with surface charge sites. The electrostatic relationship between surface charge and solute ions adsorbed is visualized as similar to that of plates of an electrical capacitor. The properties of a surface that need consideration in using this model include the surface charge σ_s, which can be ions of specified charge per unit area, and the surface potential ψ_s, which is a measure of the influence of solute ions, particularly H^{+} and OH^{-}, on adsorption. Also significant are the dielectric constants of the solution and the solvent adjacent to the surface.

This model offers a means of evaluating the adsorbing properties of solid surfaces in a rather specific fashion, and a large number of research studies have utilized it. The review by James and Parks (1982) cites many papers that are relevant to studies of adsorption by surfaces in aqueous systems.

One of the more successful models based on double-layer theory and used for describing the amount of adsorption of heavy metals on a pure silica surface (finely divided quartz) has been proposed by James and Healy (1972). This model describes the adsorption of cations on quartz or silicate surfaces by means of a Langmuir isotherm. The adsorption of a cation i^{+z} to the fraction of available surface $1-\Theta$ results in a fraction of surface denoted by θ_i to which the cation is adsorbed. The sum of the individual θ_i values is equal to the fraction of surface to which all solutes are adsorbed. The equilibrium expression for a cation can be thought of as describing the reaction:

$$i^{+z} + (1-\Theta)[\text{available sites}] \leftrightharpoons \theta_i[\text{occupied sites}] \qquad (20)$$

and

$$K_i^{ads} = \frac{\theta_i}{[i^{+z}]\ (1-\Theta)}\ . \qquad (21)$$

The equilibrium constant for this Langmuir type adsorption is related to the free energy of adsorption ΔG_i^{ads} by the standard thermodynamic relation $K_i^{ads} = e^{-\Delta G_i^{ads}/RT}$. The James-Healy model describes ΔG_i^{ads} as the sum of three free energies; the energy of coulombic attraction between the ion and the charged surface (ΔG_i^{coul}), the change in free energy resulting from replacement of the adsorbing ion's secondary hydration sheath by the adsorbing surface environment (ΔG_i^{solv}) and the remaining ("chemical") free energy of adsorption (ΔG_i^{chem}) due to covalent, Van der Waals, London dispersion, and other attractive forces, many of which do not easily lend themselves to theoretical interpretation.

Although some models exist whereby the "chemical" adsorption term may be estimated from cation-silicate ion equilibria (Schindler and others, 1976), extrapolation to mineral surfaces more complex than simple oxides is questionable. Since there seems to exist no workable theoretical method for calculating the effects of these miscellaneous "chemical" forces for dissolved ions adsorbing to a charged surface, the "chemical" term is determined experimentally by fitting the model to experimental data after allowing for the calculated effect of ΔG_i^{coul} and ΔG_i^{solv}. Although this "chemical" term is often greater in magnitude than the pH dependent term that takes into account coulombic interaction, the latter is more important when the effect of

pH on adsorption is to be considered. For example, although the "chemical" free energy term is often highly negative as indicative of a strong adsorbing tendency (particularly for such heavy metal cations as Cu^{+2}, Ag^{+}, Hg^{+2}), a very low pH may render the surface charge sufficiently positive so as to repel and desorb such cations. Variation of the pH about this point must be fully understood in terms of its effect on the coulombic interaction which causes this. James and Healy (1972) considered the coulombic and solvation effects on adsorption for the different species of a given metal to account for all the difference between adsorption of the hydrolyzed (for example, $PbOH^{+}$, $Pb(OH)_3^-$, and so on) and unhydrolyzed (for example, Pb^{+2}) species. For this reason, the "chemical" contributions to the adsorptive free energy are considered to be equal for hydrolyzed and unhydrolyzed forms.

In deriving the term for the coulombic free energy, it is assumed that the chemical attraction of H^+ or OH^- ions to discrete adsorption sites on an oxide surface gives rise to a positive surface charge when the adsorption density Γ_{H^+} of H^+ ions is larger than the adsorption density "Γ_{OH^-}" of sites at which an H^+ has been released from a water molecule; the converse, of course, produces a negative surface charge.

It should be noted that H^+, but not OH^-, ions are believed to actually adsorb to surface-bound hydroxyl groups (thereby establishing a surface charge) in the surface reaction:

$$\gtrless S\text{–}OH + H^+ \leftrightharpoons \gtrless S\text{–}OH^+ \qquad (22)$$

where $\gtrless S-$ represents a lattice atom (probably Si or Al) to which is bound a hydroxyl group as a result of the initial reaction with water when the material was first placed in contact with it. The same is not quite true with regard to OH^- ions. It is generally believed that instead of adsorbing to a surface hydroxyl group, an aqueous OH^- ion near the surface will remove a hydrogen from the surface-bound hydroxyl, leaving behind a negatively charged oxygen atom; the purported reaction is written:

$$\gtrless S\text{–}OH + OH^- \leftrightharpoons \gtrless S\text{–}O^- + H_2O \qquad (23)$$

For convenience, however, the notation relating to the setting up of negative charge in the above reaction will be noted as though OH^- adsorption were really occurring; the surface coverage for which the above reaction has occurred will therefore be called Γ_{OH^-}.

The net surface charge density σ_s is given by

$$\sigma_s = F(\Gamma_{H^+} - \Gamma_{OH^-}), \qquad (24)$$

where F is the Faraday constant, equal to 96,490 coulombs of electrical charge per mole of hydrogen ions. There exists for each type of mineral surface a pH which is characteristic of the particular surface at which the H^+ and OH^- adsorption densities are equal so that σ_s equals zero in the ideal case of an "inert" nonadsorbing background electrolyte. This pH is called the point of zero charge (pH_{pzc} or PZC), above which OH^- ions interact preferentially over H^+ ions, giving rise to a net negative surface charge, and below which H^+ ions adsorb preferentially over OH^-, giving rise to a positive charge.

James and Healy (1972) state that the potential, ψ_s, at the surface, due to adsorbed H^+ and OH^- ions, decreases by 59 millivolts (mV) per unit of increased pH at 25°C, and is given by the Nernst equation in the form:

$$\psi_s = \frac{2.303RT}{|z|\,F}(pH_{pzc} - pH). \qquad (25)$$

The variable $|z|$ is the electrolyte valence number which is 1 for uni-univalent salts such as NaCl, $\sqrt{2}$ for uni-divalent salts such as $CaCl_2$ or Na_2SO_4, and 2 for di-divalent salts such as $MgSO_4$. In order to understand how the potential varies with distance from the surface, it is necessary to understand the effect of the electrical charge within the region from the surface to a given distance. The surface charge density σ_s is electrically balanced in part by a diffuse layer of charge σ_d in the electrolyte solution. The distribution of supporting electrolyte ions near the surface is such that those ions of charge opposite in sign to surface charge density σ_s tend to be attracted toward the surface while those of similar charge sign tend to be repelled. The result is an increment of the diffuse charge density σ_d located in the first molecular layer of solute and opposite in sign to the surface density. This is followed in successive increments of solution at increasing distances from the surface by successively smaller diffuse charge increments until the total diffuse layer charge density is equal in magnitude (and opposite in sign) to the surface charge density. The diffuse layer charge density, within the region from the surface to the distance at which cations may adsorb, affects the extent to which the potential at that distance differs from the surface potential. Since this potential depends on the presence of cations and anions of the supporting electrolyte, the magnitude of the diffuse layer charge is dependent on the ionic strength of the solution. Using the assumption of a dielectric constant independent of distance from the surface (and equal to the dielectric constant of pure water, 78.5 at 25°C), it can be shown that the value of the diffuse-layer charge density σ_d is proportional to the square root of the ionic strength μ of the supporting electrolyte and, furthermore, that the decay of the surface potential σ_s as a function of distance x_i from the surface will give a distance-dependent potential ψ_{x_i} described by the relation:

$$\psi_{x_i} = \frac{2RT}{zF} \ln \frac{(e^{zF\psi_s/2RT}+1)+(e^{zF\psi_s/2RT}-1)e^{-Bx_i\sqrt{\mu}}}{(e^{zF\psi_s/2RT}+1)-(e^{zF\psi_s/2RT}-1)e^{-Bx}} \qquad (26)$$

where B is the same constant used in the extended Debye-Huckel equation for ionic activity coefficients, and is equal to $0.3286\times10^{10}\text{m}^{-1}\text{mol}^{-\frac{1}{2}}\text{dm}^{\frac{3}{2}}$, and μ is the ionic strength. (For simplified calculations, taking B as 0.3286 and using Angstrom units for x_i, and moles per liter for ionic strength seems preferable to using more cumbersome SI units.) James and Healy (1972) used for x_i (the hydrated radius and distance of closest approach of the adsorbed ion) the sum of the crystal ionic radius plus the diameter of a molecular layer of water (taken as 2.76 Å) presumed to form a nonremovable primary hydration sheath. The change in free energy due solely to electrostatic interaction (ΔG_i^{coul}) between the charged surface adsorbing ion i will be equal to

$$\Delta G_i^{coul} = z_i F \psi_{x_i} , \qquad (27)$$

where z_i is the ionic charge and ψ_{x_i} is the potential acting at distance x_i from the surface. That change in free energy adsorption then, which is due solely to the change in the electrostatic environment, is—according to the James-Healy model—a function of pH and ionic strength. Figure 1 shows how ΔG_i^{coul} for both the Pb^{+2} and $\Delta G_{PbOH^+}^{coul}$ ions varies in this model as a function of the difference between the pH and pH_{pzc} at various ionic strengths.

The dielectric constant or electrostatic permittivity of the surface micro-environment is different from that of the bulk water because of the replacement, upon adsorption, of adsorbed ions' outer hydration sheaths with the water molecules that are attached to the surface. The consequence of this is that an adsorbed ion will be energetically different from the same dissolved ion; the energy required to remove from a dissolved cation the part of the hydration sheath that is removed upon adsorption will not be balanced by the energy released when the ion becomes adsorbed to the surface. This is true because the dielectric constant of the water molecules at the surface, and of the surface itself, are different from those of the water molecules formerly in the hydration sheath. The expression given by James and Healy (1972) for the change in free energy of adsorption (ΔG_i^{solv}), due to this effect is

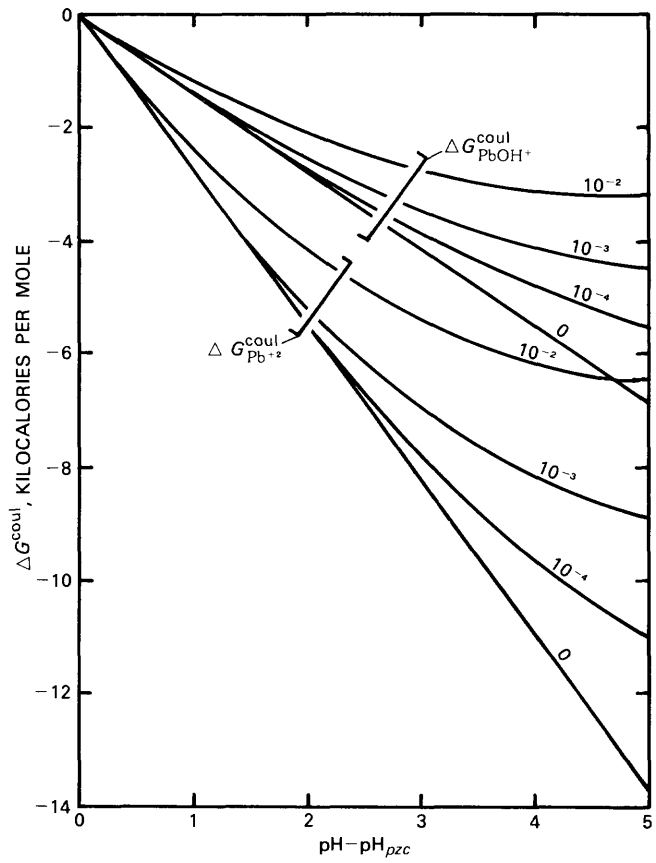

Figure 1. Variation of coulombic terms $\Delta G^{coul}_{PbOH^+}$ and $\Delta G^{coul}_{Pb^{+2}}$ of the free energy of adsorption with pH and ionic strength.

Here, N_0 is Avogadro's number, 6.023×10^{23} mol^{-1}, e is the electronic charge, 0.16022×10^{-18} C, r_i is the crystal ionic radius of the unhydrated ion, and ϵ_0 is the permittivity constant of free space, equal to $8.85411\times10^{-12}\text{C}^2N^{-1}\text{m}^{-2}$. The dielectric constants are denoted by ϵ_{H_2O} for water, ϵ_{solid} for the solid adsorbent, and ϵ_{int} for the interfacial region between the surface and the center of the adsorbed ion. For this latter value, James and Healy (1972) give the empirical relation:

$$\epsilon_{int} = \frac{\epsilon_{H_2O}^{-6}}{1+(1.2\times10^{-17})(d\psi/dx)^2} + 6, \qquad (29)$$

where $d\psi/dx$ is the electric field strength at the surface in volts per meter, and ϵ_{H_2O} is 78.5, water's dielectric

$$\Delta G_i^{solv} = \left(\frac{z_i^2e^2N_0}{16\pi\epsilon_0}\right)\left(\frac{1}{x_i}\right) - \left(\frac{r_i}{2x_i^2}\right)\left(\frac{1}{\epsilon_{int}} - \frac{1}{\epsilon_{H_2O}}\right) + \left(\frac{z_i^2e^2N_0}{32\pi\epsilon_0}\right)\left(\frac{1}{x_i}\right)\left(\frac{1}{\epsilon_{solid}} - \frac{1}{\epsilon_{int}}\right) . \qquad (28)$$

constant at 25°C under zero applied electric field. The field strength $d\psi/dx$ at the center of the adsorbed ion is estimated from the Gouy-Chapman model of the double layer by the relation:

$$\frac{d\psi}{dx} = -2B\sqrt{\mu}\,\frac{RT}{|z|F}\sinh\left(\frac{|z|F\Delta\psi x_i}{2RT}\right). \quad (30)$$

The change in free energy due to solvation effects, then, is a function of ϵ_{int}, which is in turn, a function of $d\psi/dx$ and hence of ψ_{x_i} in the James-Healy model.

There is some uncertainty with regard to the correct expression for the change in the free energy of solvation. The expression (eq 28) given by James and Healy (1972) for ΔG_i^{solv} was refined (prior to the 1972 publication date) by Levine (1971). Levine's model, according to Wiese, James, and Healy (1971), constitutes a more accurate and rigorous theoretical analysis of the changes in solvation energy that accompany adsorption, and is given as

$$\Delta G_i^{solv} = \frac{1}{2} z_i e N_0 \Phi + \frac{z_i^2 e^2 N_0}{8\pi\epsilon_0 x_i}\left(\frac{1}{\epsilon_{int}} - \frac{1}{\epsilon_{H_2O}}\right). \quad (31)$$

The term Φ is the electrostatic potential at the center of the adsorbed ion and results from electrostatic images in two places of dielectric discontinuity, namely, the solid-interface and solution-interface boundaries, and is given by

$$\Phi = \left(\frac{z_i e}{8\pi\epsilon_0}\right)\left(\frac{1}{\epsilon_{int}}\right)\left(\frac{1}{x_i}\right) \times \left[\frac{(f_1+f_2)}{|f_1 f_2|^{1/2}}\tan^{-1}|f_1 f_2|^{1/2} - \ln(1+|f_1 f_2|)\right], \quad (32)$$

where

$$f_1 = \frac{\epsilon_{int} - \epsilon_{solid}}{\epsilon_{int} + \epsilon_{solid}} \quad (33)$$

and

$$f_2 = \frac{\epsilon_{int} - \epsilon_{H_2O}}{\epsilon_{int} + \epsilon_{H_2O}}. \quad (34)$$

The complete expression for the improved ΔG_i^{solv} term is therefore

$$\Delta G_i^{solv} = \left(\frac{z_i^2 e^2 N_0}{16\pi\epsilon_0}\right)\left(\frac{1}{\epsilon_{int}}\right)\left(\frac{1}{x_i}\right)\left[\frac{(f_1+f_2)}{|f_1 f_2|^{1/2}}\tan^{-1}|f_1 f_2|^{1/2} - \ln(1+|f_1 f_2|)\right] + \left(\frac{z_i^2 e^2 N_0}{8\pi\epsilon_0}\right)\left(\frac{1}{x_i}\right)\left(\frac{1}{\epsilon_{int}} - \frac{1}{\epsilon_{H_2O}}\right) \quad (35)$$

As with the ΔG_i^{solv} expression given by James and Healy (1972), Levine's (1971) expression is also dependent on the interfacial dielectric constant ϵ_{int} for the region between the adsorbing solid and the bulk solution. Figure 2 shows how James and Healy's (1972) and Levine's expressions for $\Delta G_{Pb^{+2}}^{solv}$ and $\Delta G_{PbOH^+}^{solv}$ vary with ϵ_{int}. The Levine (1971) expression shows a very critical dependence on ϵ_{int} which may have a profound effect on the relative magnitudes of adsorption of Pb^{+2} and $PbOH^+$. If, at one extreme, ϵ_{int} were to equal 6 (the lower limit of the dielectric constant of water), figure 2 shows that the ΔG_i^{solv} values for Pb^{+2} and $PbOH^+$ adsorption on quartz would be 14.70 and 3.68 Kcal/mol, respectively. This means that 11 Kcal/mol more energy is required to remove the secondary hydration sheath from Pb^{+2} than from $PbOH^+$ prior to adsorption. This very large difference could lead to preferential adsorption of $PbOH^+$ over Pb^{+2} even if the aqueous activity of Pb^{+2} greatly exceeded that of $PbOH^+$, which rarely happens in natural waters of moderate pH. At the other extreme, if ϵ_{int} were to equal 78.5, the value for water, figure 3 shows $\Delta G_{Pb^{+2}}^{solv}$ and $\Delta G_{PbOH^+}^{solv}$ values of 0.90 and 0.22 Kcal/mol, respectively. Here, a mere 0.7 Kcal/mol more energy would need to be supplied to Pb^{+2} than to $PbOH^+$ in order to change the ion's solvation environment prior to adsorption. This would be more than offset above the pH_{pzc} by the fact that the coulombic attraction would be twice as large for Pb^{+2} as for $PbOH^+$. For example, if the pH were 2 units above the pH_{pzc}, the values of $\Delta G_{PbOH^+}^{coul}$ at zero ionic strength (fig. 1) would be −5.46 and −2.73 Kcal/mol, respectively, so that the sum of the coulombic and solvation contributions to the free energy of adsorption would be −4.56 Kcal/mol for Pb^{+2} and −2.51 Kcal/mol for $PbOH^+$. The result would be a preferential adsorption of Pb^{+2} over $PbOH^+$, even in some cases where the aqueous $PbOH^+$ activity exceeded that of aqueous Pb^{+2}. Clearly, the proper determination of the interfacial dielectric constant is quite important in allowing us to understand the actual chemical processes occurring at the surface.

As noted by Hasted, Ritson, and Collie (1948), many investigators have suggested that the dielectric constant of a layer of water molecules tends to decrease as the molecules become more electrostatically or otherwise bound to a charged ion or surface, the lower limit being approximately 6. Bockris, Devanthan, and Muller (1963) did assign this lower limit to the dielectric constant of the first water layer adsorbed on the surface. The value appropriate for use in the solvation free energy charge ex-

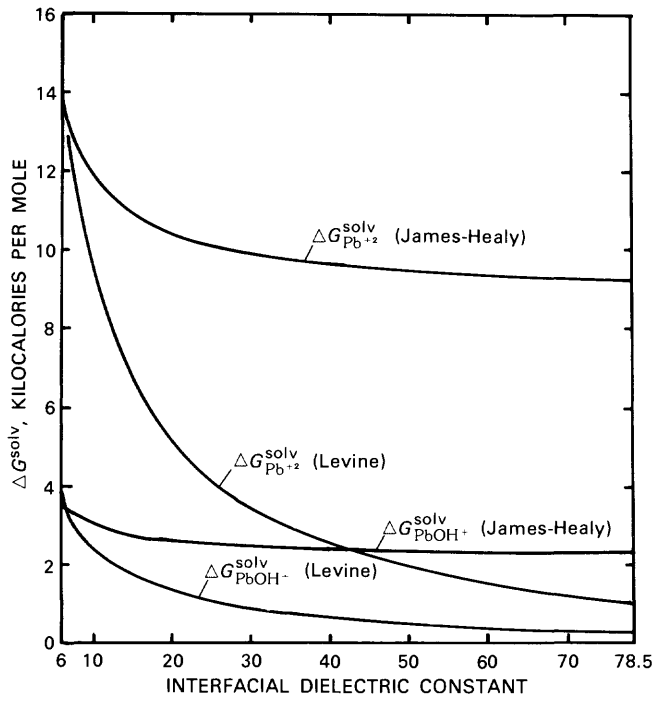

Figure 2. Variation of Levine's (1971) and James and Healy's (1972) expressions for Pb^{+2} and $PbOH^+$ solvation energy for adsorption on quartz, with interfacial dielectric constant.

pression, however, would seem to be some "average" dielectric constant over the distance between the center of the adsorbing lead ion and the surface. This would include the dielectric constant contribution of water molecules surrounding the adsorbed ion ($\epsilon=6$, according to Hasted, Ritson, and Collie, 1948) and some of the bulk solute molecules ($\epsilon=78.5$) which exist in that region. Levine (1971) suggested, on the other hand, that the mean value for use in his ΔG_i^{solv} expression should lie somewhere between 30 and 40.

In light of equation 29, however, the mean dielectric constant value should depend on the electric field strength distribution within the region; it will also be dependent on the adsorbed ion density since the primary hydration sheaths of adsorbed ions have dielectric constants of 6. It, therefore, would seem unlikely that the proper value of ϵ_{int} would lie between 30 and 40 under all conditions. We may have to be content with using for ϵ_{int} whichever value between 6 and 78.5 best describes the experimental results to follow.

Variable Surface Charge—Variable Surface Potential Model

The model proposed by James and Healy (1972) makes use of the assumption that the surface potential varies in a Nernstian fashion with the solution pH. Various workers have noted that this is a poor approximation under certain circumstances. Instead of using this approximation, Bowden, Posner, and Quirk (1977) and Davis, James, and Leckie (1978) proposed models in which the surface charge σ_s is produced as the result of a chemical interaction between surface sites specific for adsorption and desorption of the potential-determining H^+ ions. The diffuse layer charge σ_d is given as a function of ionic strength and surface potential ψ_d (analogous to ψ_{x_i} in the James-Healy model). The remaining charge required to give overall electroneutrality is the positive charge density σ_i of the adsorbed cations other than H^+ (whose effect is already accounted for in the expression for). The potential ψ_d, acting upon the adsorbing ions, gives rise to the coulombic free energy terms (in our case $\Delta G^{coul}_{Pb^{+2}}$ and $\Delta G^{coul}_{PbOH^+}$)which, if negative in sign (along with ψ_d) tend to promote adsorption subject to other free energy contributions.

This model is referred to by Bowden, Posner, and Quirk (1977) as the variable-surface-charge/variable-surface-potential (VSC−VSP) model in order to emphasize the fact that both surface charge and surface potential are dependent on pH, ionic strength, and other solution parameters.

The protonation and deprotonation of neutral surface sites to give a charged surface are represented in this model as in equations 22 and 23. The Langmuir-like expressions for adsorption equilibrium will be written:

$$K'_{H^+} = \frac{\{\equiv S\text{–}OH_2^+\}}{\{\equiv S\text{–}OH\}\,[H^+]} = \frac{\Gamma_{H^+}}{(N_s - \Gamma_{H^+} - \Gamma_{OH^-})\,[H^+]} \qquad (36)$$

and

$$K'_{OH^-} = \frac{\{\equiv S\text{–}O^-\}}{\{\equiv S\text{–}OH\}\,[OH^-]} = \frac{\Gamma_{OH^-}}{(N_s - \Gamma_{H^+} - \Gamma_{OH^-})\,[OH^-]} \qquad (37)$$

where the quantities in braces ({ }) represent surface concentrations of the occupied and therefore charged sites in the numerators and of the unoccupied sites in the denominators. The surface concentrations may also be expressed as moles per square meter of adsorbed H^+ or OH^-, represented by Γ_{H^+} and Γ_{OH^-}.

K'_{H^+} and K'_{OH^-} are overall adsorption constants for H^+ and OH^- ions and include both chemical, solvation,

and electrostatic contributions. The value N_s is the maximum adsorption density obtainable on a given surface. Bowden, Posner, and Quirk (1977) gave an upper limit for this value of 10^{-5} equivalents of adsorption sites per square meter; a larger value would require charged sites to be less than 5Å apart and lateral coulombic repulsion forces would tend to drive them farther apart.

Equations 36 and 37 may be combined and rearranged to give the following expressions for the adsorption densities of the potential-determining ions H^+ and OH^-:

$$\Gamma_{H^+} = N_s \frac{K'_{H^+}[H^+]}{1+K'_{H^+}[H^+]+K'_{OH^-}[OH^-]} \qquad (38)$$

and

$$\Gamma_{OH^-} = N_s \frac{K'_{OH^-}[OH^-]}{1+K'_{H^+}[H^+]+K'_{OH^-}[OH^-]} \qquad (39)$$

The electrostatic interactions included in the "constants" K'_{H^+} and K'_{OH^-} arise because the adsorption of potential-determining ions (p.d.i.) gives rise to a surface charge density σ_s, which causes an opposing potential ψ_s. The adsorption of H^+, for example, will cause a positive surface charge density σ_s and positive potential ψ_s, which will tend to restrict further H^+ adsorption. This type of electrostatic effect can be separated out of the K'_{H^+} and K'_{OH^-} terms by the relations:

$$K'_{H^+} = K_{H^+} e^{-F\psi_s/RT} \qquad (40)$$

and

$$K'_{OH^-} = K_{OH^-} e^{+F\psi_s/RT} . \qquad (41)$$

Substitution of equations 38 through 41 into equation 24 for the surface charge density σ_s gives

$$\sigma_s = \frac{FN_s\{K_{H^+}[H^+]e^{-F\psi_s/RT} - K_{OH^-}[OH^-]e^{+F\psi_s/RT}\}}{1+K_{H^+}[H^+]e^{-F\psi_s/RT}+K_{OH^-}[OH^-]e^{+F\psi_s/RT}}, \qquad (42)$$

which is the first major equation of the VSC–VSP model.

By definition, the pH_{pzc} is that pH at which the surface charge density σ_s, and therefore ψ_s, are equal to zero, making all the above exponential terms equal to unity. The numerator of the above expression must equal zero at a pH equal to the pH_{pzc}, and K_{H^+} and K_{OH^-} will be related by

$$K_{H^+}[H^+_{pzc}] = K_{OH^-}[OH^-_{pzc}], \qquad (43)$$

where $[H^+_{pzc}]$ and $[OH^-_{pzc}]$ are the H^+ and OH^- activities at the pH_{pzc}. Given the ion product expression $K_w = [H^+][OH^-]$ for water, the above expression can be rearranged to give

$$K_{H^+} = \frac{K_{OH^-}K_w}{[H^+_{pzc}]^2} = \frac{K_{OH^-}K_w}{(10^{-pH_{pzc}})^2} . \qquad (44)$$

Given the pH_{pzc}, only K_{H^+} (or K_{OH^-}, but not both) is necessary in order to fully describe the interaction of H^+ and OH^- with the surface. This often-used approach, however, is somewhat backward, for it is really the relative chemical affinities (as expressed by K_{H^+} and K_{OH^-}) of H^+ and OH^-, for the surface reactions previously mentioned, that determine the value of the pH_{pzc}, as described by

$$pH_{pzc} = \tfrac{1}{2} \log_{10}\left\{\frac{K_{H^+}}{K_w K_{OH^-}}\right\}, \qquad (45)$$

where K_w is the ionization constant of water, equal to 1.0×10^{-14} at 25°C.

Adsorption of ions other than potential-determining ions is viewed in the VSC–VSP model as taking place at a plane a distance d from the surface of potential-determining ion adsorption. The electrostatic potential ψ_d at this plane is related to the surface potential ψ_s by

$$\psi_s - \psi_d = \frac{\sigma_s}{G} = \frac{\sigma_s d}{\epsilon\epsilon_0} \qquad (46)$$

where G is the differential capacity of the double layer in farads ler square meter. This value is dependent on the distance d and on the effective dielectric constant ϵ from the surface out to distance d. (In this context, d and ϵ have essentially the same respective meaning as do the x_i used in the coulombic free energy term and the mean interfacial dielectric constant ϵ_{int} as used in Levine's solvation free energy term.) The potential is, therefore, assumed in this model to vary linearly with distance within the first layer of the diffuse layer.

The adsorbed cations give rise to a charge density σ_i which, with σ_d opposes σ_s (in the usual case where cations adsorb onto a negatively charged surface) and

which for lead adsorption (where both Pb^{+2} and $PbOH^+$ cations are adsorbed) is equal to

$$\sigma_i = F(2\Gamma_{Pb^{+2}} + \Gamma_{PbOH^+}), \quad (47)$$

where $\Gamma_{Pb^{+2}}$ and Γ_{PbOH^+} are the respective adsorption densities of Pb^{+2} and $PbOH^+$ in moles per square meter.

From this point on, the model is very similar to that proposed by James and Healy (1972); the change in free energy due to adsorption and resulting from the earlier-discussed chemical and solvation effects is considered, as is the coulombic contribution which can be expressed:

$$\Delta G_i^{coul} = z_i F \psi_d, \quad (48)$$

where ψ_d is analogous to ψ_{x_i} in the James-Healy model. As in that model, the total free energy of adsorption ΔG_i^{ads}, gives rise in the VSC–VSP model to an adsorption constant K_i^{ads}, which describes the Langmuir adsorption of the adsorbing ion on the surface.

The remaining charge density σ_d is that which exists in the diffuse layer of solution near the surface as a result of the distribution of electrolyte ions so as to oppose the combined charge densities σ_s and σ_i. This diffuse charge density, σ_d, is given by the relation:

$$\sigma_d = -\sqrt{8000 \epsilon_0 \epsilon_{H_2O} RT\mu} \sinh\left(\frac{|z| F \psi_d}{2RT}\right). \quad (49)$$

The final constraint of this model is that the sum $\sigma_s + \sigma_i + \sigma_d$ of the individual charge densities be equal to zero for overall electroneutrality.

In order to solve the simultaneous equations 42 and 46 through 49, we begin with an estimated value of ψ_s from which σ_s can be extracted using equation 42. With both σ_s and ψ_s, then, one can calculate ψ_d using equation 46. This value may be substituted into equation 49 to obtain σ_d, and also may be used in equation 48 to calculate the coulombic free energy term ΔG_i^{coul}. Once the solvation and "chemical" free energy terms for the adsorbing species are known, the total change in free energy on adsorption ΔG_i^{ads} and hence the adsorption equilibrium constant K_i^{ads} may be calculated and substituted into the appropriate equilibrium expression similar to equations 38 and 39 (but for adsorbing non-p.d.i. species) in order to yield the adsorbed species concentration Γ_i. Given the appropriate adsorption densities, the charge density σ_i due to this adoption can be calculated; if the sum $\sigma_s + \sigma_i + \sigma_d$ of the charge densities calculates as greater than zero, the original estimate of σ_s was too high and should be reduced in some proportion to the error generated. Conversely, if the sum is less than zero, σ_s should be increased. The iteration is continued until the sum of σ_s, σ_i, and σ_d is within predefined tolerance limits, very nearly equal to zero.

Figure 3 is a schematic representation of the double-layer model with a univalent adsorbed cation at a pH high enough above the pH_{pzc} so as to render the surface charge σ_s and potentials ψ_s and ψ_d negative.

In summary, the VSC–VSP model may be an improvement over that of James and Healy (1972) insofar as it avoids the assumption that the surface potential exhibits Nernstian behavior with respect to pH. The surface potential is instead calculated so as to consider the effect of adsorbed cations themselves, and to recognize potential-determining ions as having finite sizes and hence finite maximum surface densities.

In the following sections of this paper, the VSC–VSP model will be applied to a characterization of a natural stream sediment fraction and will be tested by observing the interaction between the sediment and dilute aqueous solutions containing lead.

COMPLEX ION FORMATION AND PRECIPITATE SOLUBILITY

Lead forms complexes with the various inorganic anions, such as chloride, fluoride, carbonate, bicarbonate, and hydroxide. These anions tend to increase aqueous lead concentrations by binding aqueous lead, keeping it in solution, but preventing it from taking part in other chemical reactions (primarily adsorption) that would otherwise reduce its concentration. This effect is opposed by the tendency of some complexes, such as $PbOH^+$, to adsorb as well. Lead also forms complexes with organic ligands; it may be mobilized by attachment to dissolved organic chelating agents while also being immobilized by attachment to organic polymeric material, such as soil humus. The latter process is more nearly analogous to precipitation, as the humic material has generally a low solubility in water and remains attached to soil particles. Organic complexing effects, however, are not considered in this paper, that subject being a separate field by itself. The predominantly important inorganic complexes of lead in natural water systems are those of hydroxide and carbonate. Sulfate and chloride complexes may occur in some waters, particularly in saline estuarine waters or in the ocean itself. The known monomeric hydroxy complexes are $PbOH^+$, $Pb(OH)_3^-$, and $Pb(OH)_4^{-2}$, the most important of these being $PbOH^+$. The latter two complexes become significant only above the pH of most natural waters, and because $PbOH^+$, a cation, will likely be more readily adsorbed to negatively charged surfaces than will be the anions $Pb(OH)_3^-$ and $Pb(OH)_4^{-2}$, assuming that the chemical terms are the same (as was suggested by James and Healy, 1972) for all species of the same element.

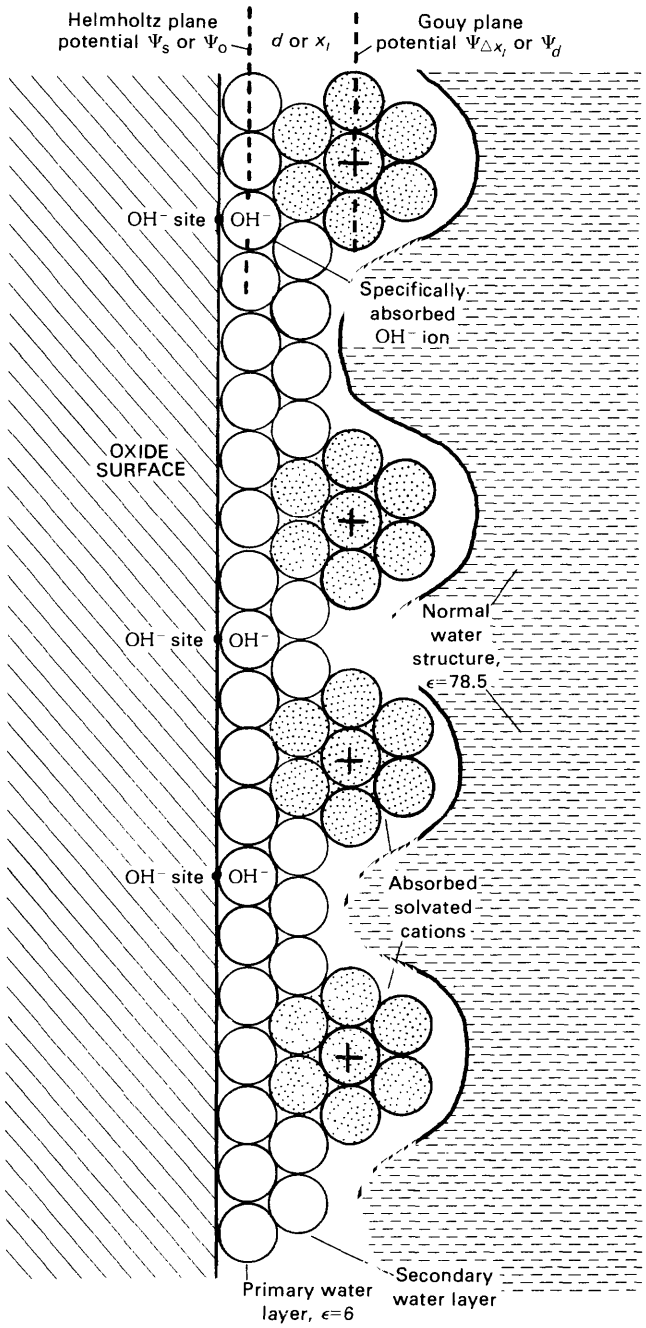

Figure 3. Schematic representation of adsorbed cations at inner double layer.

Lead also forms a series of polymeric hydroxide complexes, a tendency displayed by many other metal ions. These can probably be viewed as solid-phase precursors in the sense of having a definite structural pattern; they are, however, of significant importance only in solutions having rather high total dissolved concentrations of the metal. Baes and Mesmer (1976) prepared a critical review of metal ion hydrolysis data, and noted that polymeric forms of lead hydroxide are dominant between pH 6.0 and 10.0 only when total lead concentration exceeds 0.1 molar, but only monomers are significant if total dissolved lead is 10^{-5} molar. Any polymeric hydroxide complexes containing many Pb^{+2} ions that will form will approach the composition of $Pb(OH)_2^0$ and may be indistinguishable from this uncharged ion.

In natural aqueous systems, lead will be present in very low concentrations and polynuclear complexes will be present in insignificant amounts. Thermodynamic data for the monomeric species indicate that Pb^{+2} should predominate up to about pH 7.0 and $PbOH^+$ should predominate in the pH range of 7 to 9. The $Pb(OH)_2^0$ species (if it exists, or a polymer approximating that composition) calculates as significant in the 9 to 12 pH range. Though the existence of this species may be in doubt, the use of a $Pb(OH)_2^0$ term in the overall solubility equation may be of value in approximating the magnitude of the effect of polynuclear species interpreted to be $Pb(OH)_2^0$. The carbonate ion pair $PbCO_3^0$, and $Pb(CO_3)_2^{-2}$ may become significant above pH 5 and may become significant where the total carbonate in the system exceeds the dissolved lead, as is almost always the case in natural waters. The formation constants given by Lind (1978) (and written in terms of H^+ rather than OH^- ion[1]) for $PbOH_2^0$, $Pb(OH)_2$, and $Pb(OH)_3$ are, respectively, $10^{-7.23}$, $10^{-16.93}$, and $10^{-28.11}$; that for the formation of $Pb(OH)_4$ is given by Hem (1976) as $10^{-39.70}$. Also given are the first and second lead carbonate complex constants as $10^{7.24}$ and $10^{10.64}$, respectively, as determined by Bilinski and Stumm (1973). Figure 4 shows a pH–ΣCO_2 diagram based on these constants which gives the areas of predominance for the Pb^{+2}, $PbOH^+$, $Pb(OH)_2^0$, $Pb(OH)_4^{-2}$, $PbCO_3^0$, and $Pb(CO_3)_2^{-2}$ ions.

The mass balance relationship for dissolved hydroxy and carbonate lead species contributing to total lead concentration is expressed:

$$C_{Pb} = (Pb^{+2}) + (PbOH^+) + (Pb(OH)_2^0) + (Pb(OH)_3^-) + (Pb(OH)_4^{-2}) + (PbCO_3^0) + (Pb(CO_3)_2^{-2}), \quad (50)$$

where C_{Pb} is the molar concentration of dissolved lead in any form and the terms in parentheses represent molar concentrations of the species indicated. Other terms, such as $(PbCl_4^{-2})$ or $(Pb_3(OH)_4^{+2})$, should be added if they contribute significantly to the overall lead concentration. However, in river waters, the hydroxide and carbonate complexes have the greatest effect on solubility. In terms

[1]The formation constant for the reaction $Pb^{+2} + nH_2O \rightleftharpoons Pb(OH)_n^{2-n} + nH^+$ is expressed

$$\beta_{Pb(OH)_n^{2-n}} = \frac{[Pb\ (OH)_n^{2-n}]\ [H^+]^n}{[Pb^{+2}]}.$$

of thermodynamic activities and activity coefficients, the mass balance equation above can be expressed:

$$C_{Pb} = \frac{[Pb^{+2}]}{\gamma_{Pb^{+2}}} + \frac{[PbOH^{+}]}{\gamma_{PbOH^{+}}} + \frac{[Pb(OH)_2^0]}{\gamma_{Pb(OH)_2^0}} + \frac{[Pb(OH)_3^-]}{\gamma_{Pb(OH)_3^-}} + \frac{[Pb(OH)_4^{-2}]}{\gamma_{Pb(OH)_4^{-2}}} + \frac{[PbCO_3^0]}{\gamma_{PbCO_3^0}} + \frac{[Pb(CO_3)_2^{-2}]}{\gamma_{Pb(CO_3)_2^{-2}}}, \quad (51)$$

where bracketed terms are thermodynamic activities (in moles per liter) of the species, and the gamma (γ) terms are their ion activity coefficients. For ionic strengths of less than 0.1 *M*, these activity coefficients are related to the ionic strength μ by the Debye-Hückel equation:

$$\log_{10} \gamma_i = \frac{-Az_i^2\sqrt{\mu}}{1+\mathring{a}_i B\sqrt{\mu}}, \quad (52)$$

where A and B are constants at a given temperature, z_i is the integral charge of the ion and $\mathring{a}$ is the effective diameter of the aqueous ion.

At chemical equilibrium the activities of the various species are mathematically related to the complex formation constants by the following six mass-law equations:

$$\beta_{PbOH^{+}} = \frac{[PbOH^{+}]\,[H^{+}]}{[Pb^{+2}]}, \quad (53)$$

$$\beta_{Pb(OH)_2^0} = \frac{[Pb(OH)_2^0]\,[H^{+}]^2}{[Pb^{+2}]}, \quad (54)$$

$$\beta_{Pb(OH)_3^-} = \frac{[Pb(OH)_3^-]\,[H^{+}]^3}{[Pb^{+2}]}, \quad (55)$$

$$\beta_{Pb(OH)_4^{-2}} = \frac{[Pb(OH)_4^{-2}]\,[H^{+}]^4}{[Pb^{+2}]}, \quad (56)$$

$$\beta_{PbCO_3^0} = \frac{[PbCO_3^0]}{[Pb^{+2}]\,[CO_3^{-2}]}, \quad (57)$$

and

$$\beta_{Pb(CO_3)_2^{-2}} = \frac{[Pb(CO_3)_2^{-2}]}{[Pb^{+2}]\,[CO_3^{-2}]^2}. \quad (58)$$

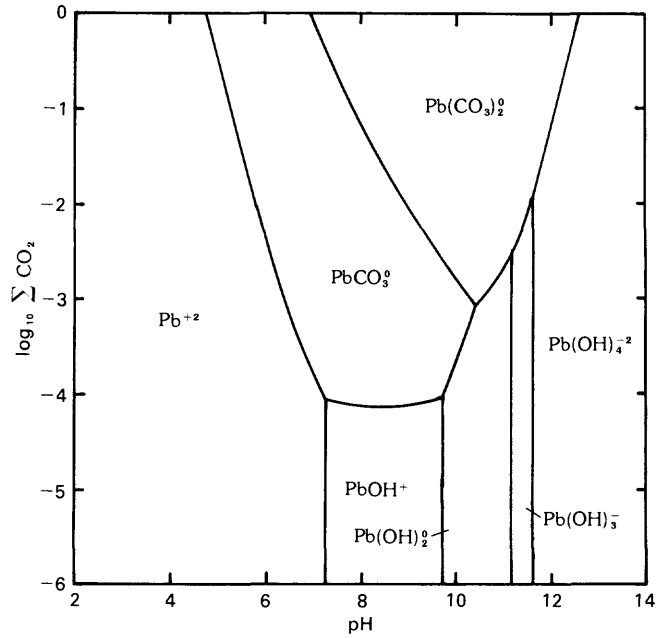

Figure 4. Plot of predominant aqueous hydroxide and carbonate complexes of lead as a function of pH and dissolved carbon dioxide.

These may be rearranged and substituted into equation 51 to give

$$C_{Pb} = [Pb^{+2}]\left\{\frac{1}{\gamma_{Pb^{+2}}} + \frac{\beta_{PbOH^{+}}}{[H^{+}]\gamma_{PbOH^{+}}} + \frac{\beta_{Pb(OH)_2^0}}{[H^{+}]^2\gamma_{Pb(OH)_2^0}} + \frac{\beta_{Pb(OH)_3^-}}{[H^{+}]^3\gamma_{Pb(OH)_3^-}} + \frac{\beta_{Pb(OH)_4^{-2}}}{[H^{+}]^4\gamma_{Pb(OH)_4^{-2}}} + \frac{\beta_{PbCO_3^0}[CO_3^{-2}]}{\gamma_{PbCO_3^0}} + \frac{\beta_{Pb(CO_3)_2^{-2}}[CO_3^{-2}]^2}{\gamma_{Pb(CO_3)_2^{-2}}}\right\}. \quad (59)$$

This expression permits calculation of the equilibrium solubility of lead in a system at 25°C and one atmosphere where ionic strength (and hence ion activity coefficients), pH, and a measure of dissolved carbon dioxide species are known, provided that the concentration of at least one specific form (usually Pb^{+2}) of dissolved lead is known. (A separate calculation of $[CO_3^{-2}]$ may be required, but this can be readily accomplished using iterative procedures given by Garrels and Christ, 1964, p. 76–83.)

The equilibrium activity of the free lead ion Pb^{+2} may be controlled in some waters by the solubility of solid precipitates. For example, if $[OH^-]=10^{-8}$ M (pH=6) and $[CO_3^{-2}]=10^{-4}$ M, one way to perform calculations (for which the solubility products have been calculated from the free energy data given by Hem and Durum, 1973) is as follows:

If equilibrium is controlled by solid $Pb(OH)_2$, for which the pK_{s0} (negative base 10 logarithm of solubility produce K_{s0}) is 19.84, we have

$$[Pb^{+2}] = \frac{K_{s0}}{[OH^-]^2} = \frac{10^{-19.84}}{(10^{-8})^2} = 10^{-3.84}. \quad (60)$$

If equilibrium is controlled by solid $PbCO_3$, for which the pK_{s0} is 13.42, we have

$$[Pb^{+2}] = \frac{K_{s0}}{[CO_3^{-2}]} = \frac{10^{-13.42}}{(10^{-4})} = 10^{-9.42}. \quad (61)$$

If the equilibrium is controlled by the hydroxycarbonate $Pb_3(OH)_2(CO_3)_2$, for which the pK_{s0} is 56.69, we have

$$[Pb^{+2}] = \left(\frac{K_{s0}}{[OH^-]^2[CO_3^{-2}]^2}\right)^{1/3} = \left(\frac{10^{-56.69}}{(10^{-8})^2(10^{-4})^2}\right)^{1/3} = 10^{-10.90}. \quad (62)$$

The mineral for which the lead ion activity is calculated to be smallest at equilibrium is that which is stable in relation to the other minerals and which will, therefore, control the lead solubility at the particular given values of hydroxide and carbonate. In the above example, the mineral $Pb_3(OH)_2(CO_3)_2$ does this, limiting $[Pb^{+2}]$ to $10^{-10.90}$ M. If other anions, such as fluoride, chloride, or sulfate, are present in sufficient concentration, the crystalline solids that they may form with lead should also be considered in a similar manner.

Nriagu (1974) suggested that the lead hydroxyphosphate minerals plumbogummite and pyromorphite might control lead solubility in natural systems. Calculations and data he cited indicate a lead solubility that is lower in most natural waters than for the carbonate or hydroxy-carbonate minerals of divalent lead. Whether phosphate activities in water are commonly high enough to make this equilibrium likely, however, remains uncertain.

An alternative control of lead concentration is the adsorption of lead ions by solid surfaces. As shown by Hem (1976), this type of solubility control can bring about lead concentrations that are much lower than those predicted by equilbria involving crystalline lead solids.

COLLECTION AND CHARACTERIZATION OF SEDIMENT SUBSTRATE

Collection and Determination of Size Fractions

The sediment that was used in this study was obtained from the bed of Colma Creek, near the northern boundary of San Mateo County, California. The general location of the site and major surrounding features are shown in figure 5.

Streamflow records and sediment loads for Colma Creek have been published by the U.S. Geological Survey for the period 1963–70 (U.S. Geological Survey 1974, 1976). The gaging and sediment sampling station is located in Orange Memorial Park in South San Francisco, and the drainage area above that point is 28 km^2. About two-thirds of the drainage basin is urban, but it also includes some undeveloped, rather steeply sloping land extending to the crest of San Bruno Mountain, and substantial areas of memorial parks and cemeteries. Much of the original soil in the urban area has been covered or disturbed by construction of buildings and roadways.

Runoff occurs mainly during the months of November through April. The average discharge for the period 1963–70 was 6.63 ft^3/s, and the maximum sediment concentration observed from 1965–69 was 19,800 mg/L.

The sample used in this study was obtained from the bed of Colma Creek at the Serramonte Boulevard Bridge in Colma, about 3.7 km upstream from the gaging station. Several shovels full of the bottom material were obtained and placed in a plastic container. In the laboratory, several kilograms of the material were wet sieved through a series of sieves; the fraction passing through a 200-mesh sieve (particle diameter less than 74 μm) was placed in a 1-liter graduated cylinder filled with a 1M sodium phosphate solution and shaken vigorously. The silt fraction was then allowed to settle while the finer clay particles remained dispersed. After several hours, the clay suspension was decanted and discarded. Only the silt fraction was used in these experiments so that the material could be suspended in solution with moderate mechanical agitation. The silt fraction was similar in

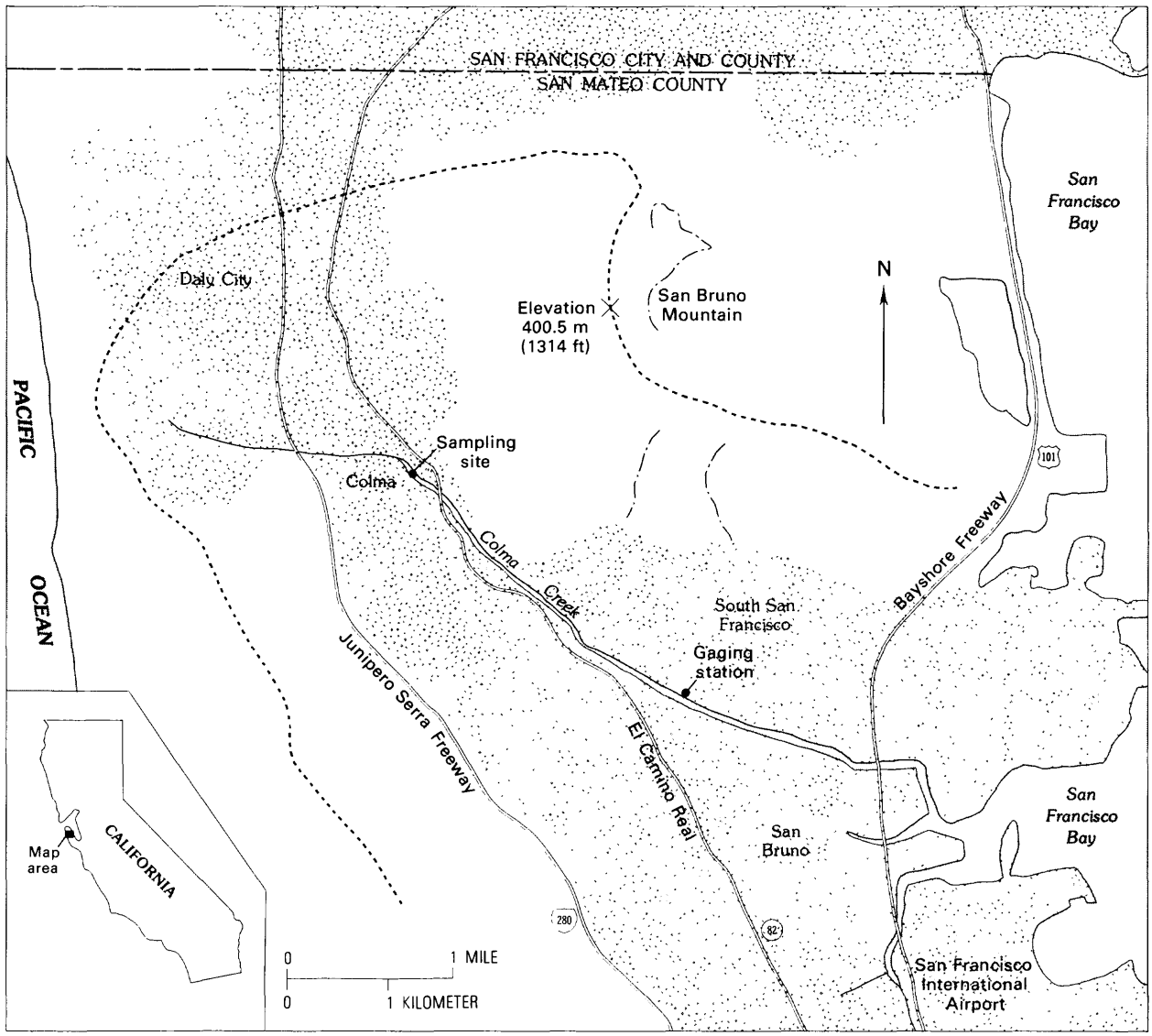

Figure 5. Drainage area of map of Colma Creek sampling site.

mineral composition to the sand fraction—consisting primarily of weathered quartz and feldspars—and was, therefore, an easily suspended indicator of the adsorption characteristics that might reasonably be expected of the sand fraction as well. Whether the behavior of clay minerals would be similar is unknown. The clay fraction was removed to simplify interpretation of the experimental results, but of course it will be necessary to study these materials also at a later time.

The data in the next column show the weight fractions and cation exchange capacity contributions of the gravel, sand, silt, and "clay" fractions of the untreated sediment sample:

Material	*Diameter (μm)*	*Cation exchange capacity meq/100 g*	*Percent by weight*	*Percent by cation exchange capacity*
Gravel	>2,000	near 0	2.6	near 0
Sand	74–2,000	3.6	94.7	72.9
Silt	4–74	32.8	1.9	13.3
"Clay"	<4	80.5	0.8	13.8

It can be seen from the data that the sediment sample taken consisted almost entirely of sand, which contributed nearly three-fourths of the total cation exchange capacity. It must be remembered, however, that in a sur-

face water environment the silt and "clay" fractions will be in closer and more direct contact with the flowing water, and the sand will be suspended for the most part only during high flows. At any rate, the X-ray diffraction patterns shown in figure 6 are nearly identical for the sand and silt fractions in that quartz and feldspar peaks predominate. The "clay" fraction, however, shows peaks for quartz, feldspars, and for chlorite-montmorillonite. (The term "clay" sometimes used by soil scientists to denote the fraction less than 4 μm in diameter is somewhat misleading; this size fraction normally includes quartz and feldspars as well as clay.)

It is beyond the scope of this paper to deal with the interaction of adsorbed heavy metals such as lead with the very complex mixture of organic matter adhering to the surface of the sediment used here. While organics-covered sediment obviously more closely approximates material encountered in nature, it is important in modeling water quality to be able to discern the separate adsorption-promoting effects of the aluminosilicate surfaces and of the organics which adhere to them. To attempt to deal with such distinct phenomena as though they were one is little better than attempting to determine a supposed "selectivity coefficient" of a shovel full of aquifer material; though such an approach might be a useful modeling tool, it yields little in the way of explanation of the underlying physical and chemical phenomena. For this reason, organic material was removed by treating the silt fraction with hydrogen peroxide for 30 minutes at 70°C in 0.3 *M* hydrochloric acid. The solids were then collected and washed repeatedly with distilled-deionized water to constant conductivity in order to remove any residual or adsorbed acid.

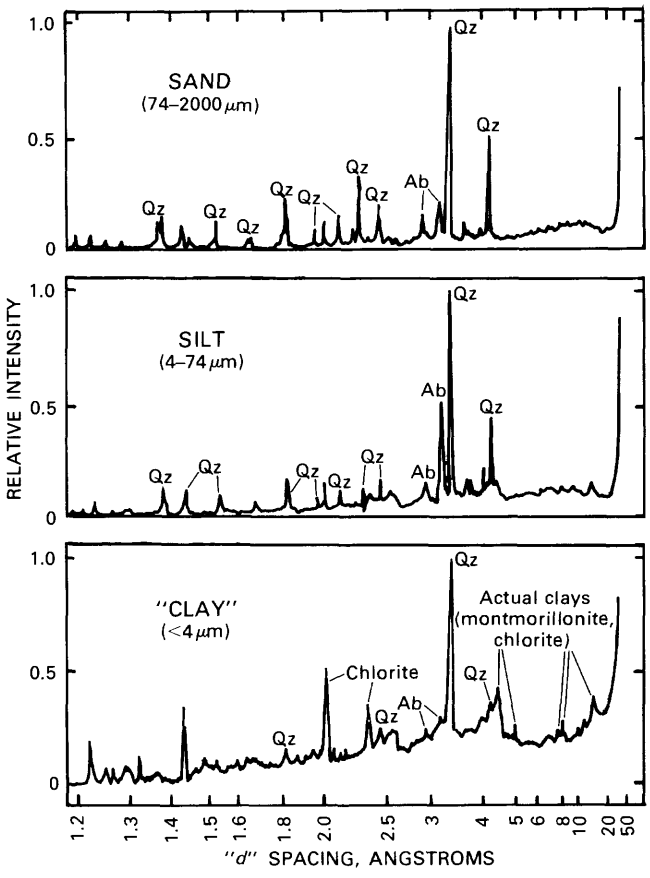

Figure 6. X-ray diffraction patterns for sand, silt, and clay fractions of Colma Creek sediment.

Surface Area and Cation Exchange Capacity

The specific surface area of the material was determined by measuring the adsorption of 1,10-phenanthroline by the material in aqueous media using Lawrie's (1961) method. The amount of 1,10-phenanthroline adsorbed by a known amount of material was determined from the final concentration of an initially saturated solution which had been shaken with the solid. From colorimetric concentration measurements of iron-complexed 1,10-phenanthroline shaken (prior to iron complexing) with various silt fraction aliquots, the specific surface area of the material was found to be 72.2 m^2/g. This is a rather large surface area for solid particles within the 4–74 μm range and may be explained in part by the extremely jagged and irregular surfaces visible under the microscopic examination.

The cation exchange capacity (CEC) per gram was measured in a manner described by Chapman (1965) in which the surface is saturated with adsorbed sodium by three successive washings with 1.0 *M* sodium acetate solution followed by three successive washings with 2-propanol in order to remove the excess sodium acetate. Finally, the adsorbed sodium was removed by washing three times with 1 *M* ammonium acetate which was collected and analyzed for sodium by atomic absorption spectrophotometry. (Each wash was followed by centrifuging for 5 minutes at 2,000 G's and decanting.) This method gave a cation exchange capacity of 3.42×10^{-4} equivalents per gram (eq/g) of the sediment, or 34.2 milliequivalents per hundred grams (meq/100 g). In terms of maximum approachable surface charge density, this is equivalent to 4.74×10^{-6} eq/m^2, which we take as the VSC–VSP parameter N_s, the maximum possible potential-determining ion adsorption density. The variable N_s is a kind of cation exchange capacity for potential-determining ions. Since ion size no doubt places an upper limit on the maximum adsorption density of either potential-determining or other adsorbed ions, and since potential-determining ions adsorb in a manner

somewhat different from that of other cations, it seems reasonable to assume that potential-determining ions and adsorbed cations might encounter altogether different adsorption maxima. Bowden, Posner, and Quirk (1977) estimated an upper limit to N_s of 1.00×10^{-5} eq/m^2 on the basis that any surface charge densities greater than this are unrealistic because centers of charge of the potential-determining ions would be less than 5 Angstroms apart and lateral coulombic forces would become excessive. (The authors refer to both surface charge density σ_s and its maximum, N_s, in terms of moles per square centimeter. Here, however, we shall, for convenience, use N_s in moles per square meter and σ_s in S.I. charge density units of coulombs per square meter; a value of 1.00×10^{-9} eq/cm^2 or 1.00×10^{-5} eq/m^2 multiplied by the Faraday of 96490 coulombs per equivalent would therefore have the same meaning as 0.965 coulombs per square meter.)

A pH_{pzc} of 4.3 was found for the adsorbent. (Details of the procedure by which this was done will be given later in this paper.) This means that within the normal pH range of most natural waters (4–9), hydroxide ion will most likely be the primary potential-determining ion. For this reason, we measured the amount of hydroxide adsorbed as a function of 1.00 N hydroxide added by titrating a 25-mL slurry of 0.292 gram (1.00×10^{-4} equiv.) of the adsorbent material with sodium hydroxide; a comparison of the conductivity (as a measure of the Na^+ and OH^- remaining in solution) to that of a blank was used to indicate the extent of hydroxide adsorption. The titration data are shown in table 1, and a plot of the moles hydroxide adsorbed (per liter of solution) as a function of hydroxide added is shown in figure 7.

As a first approximation at higher values of pH, hydroxide ion adsorption can be described by a Langmuir isotherm, such that:

$$(OH^-_{ads}) = \frac{N_s K[OH^-]}{1+K[OH^-]}, \qquad (63)$$

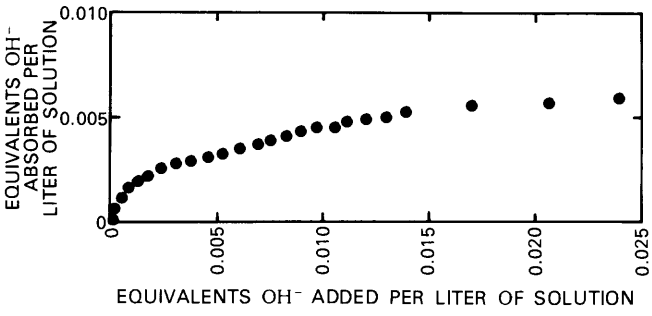

Figure 7. Adsorption of hydroxide by 0.292 grams of silt fraction of Colma Creek sediment in 25-mL volume, as function of hydroxide added.

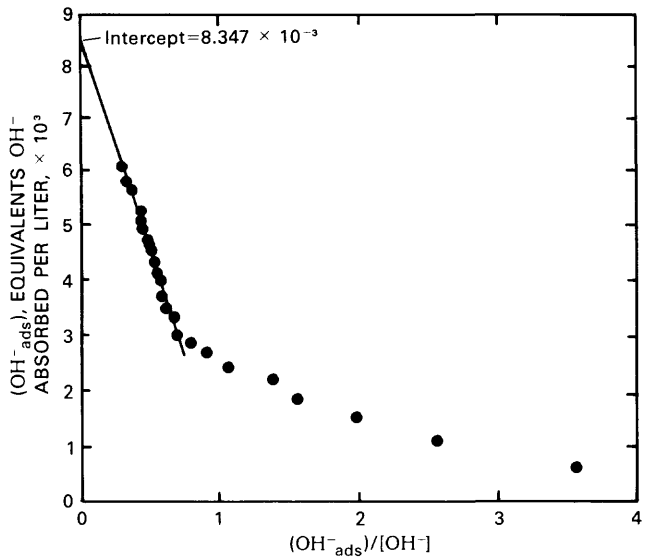

Figure 8. Langmuir plot of hydroxide adsorption on silt fraction of Colma Creek sediment.

where (OH^-_{ads}) is the adsorbed species concentration (in moles adsorbed per liter of solution) and K is an equilibrium constant which includes the $e^{+F\psi_s/RT}$ term of equation 41. If the value of ψ_s in this term is nearly constant within a given range, a plot of $(OH^-_{ads})/[OH^-]$ versus (OH^-_{ads}) should give a straight line whose intercept on the (OH^-_{ads}) axis equals N_s in concentration terms, the maximum capacity for OH^- adsorption, and whose slope equals $-1/K$; such a plot is shown in figure 8.

It can be seen from figure 8 that the data points toward the lower right of the graph for the beginning of the titration do not give a straight line, while those at the upper left for the latter half of the titration data do. The reason for this is that the pH in the latter half of the titration varied more gradually (an average of 0.05 pH unit per data point) than in the first half (0.17 pH unit per data point). Since the equilibrium "constant" K in equation 63 implicitly includes the term $e^{+F\psi_s/RT}$, and since ψ_s is a function of pH, K is a function of pH. A reasonably constant K (and hence ψ_s and pH) is necessary to give a straight-line plot. The data points from the latter portion of the titration fall in a straight line and are the most critical in determining the intercept. The least-squares intercept for the last 15 data points plotted in figure 8 (upper left of graph) is 8.35×10^{-3} eq/L, or 2.23×10^{-4} equivalents in the final volume of 26.7 mL. For the 0.292 gram adsorbent sample used, this becomes 7.63×10^{-4} eq/g (equivalents per gram) in comparison to the cation exchange capacity of 3.42×10^{-4} eq/g determined by the Chapman (1965) procedure previously described, a ratio of 2.23 to 1.

A maximum hydroxide adsorption density of 7.63×10^{-4} eq/g on an adsorbent with 72.2 m^2/g specific surface area implies a maximum surface charge density

Table 1. Determination of maximum hydroxide adsorption density by conductivity titration of 0.292 gram of adsorbent with NaOH in 25 milliliters solution

Volume (milliliters) of 1.00 N NaOH *added*	pH	*Conductivity (micromhos per centimeter)*	*Aqueous* NaOH *concentration*[1] *(moles per liter)*	*Adsorbed* NaOH *concentration*[2] *(moles per liter)*	$(OH^-_{ads})/[OH^-]$, *Adsorbed* OH^- *concentration divided by aqueous activity*[3]
0.020	10.2	35.0	1.76×10^{-4}	6.18×10^{-4}	3.56
.040	10.7	91.0	4.49×10^{-4}	1.13×10^{-3}	2.57
.060	10.9	171.1	8.08×10^{-4}	1.54×10^{-3}	1.96
.080	11.1	266.9	1.24×10^{-3}	1.86×10^{-3}	1.56
.100	11.2	372.6	1.66×10^{-3}	2.19×10^{-3}	1.38
.125	11.4	546.7	2.39×10^{-3}	2.41×10^{-3}	1.06
.150	11.5	715.3	3.10×10^{-3}	2.66×10^{-3}	.912
.175	11.6	892.4	3.85×10^{-3}	2.86×10^{-3}	.794
.200	11.7	1073	4.66×10^{-3}	3.00×10^{-3}	.693
.225	11.7	1222	5.30×10^{-3}	3.31×10^{-3}	.675
.250	11.8	1404	6.08×10^{-3}	3.48×10^{-3}	.622
.275	11.8	1576	6.84×10^{-3}	3.67×10^{-3}	.586
.300	11.9	1726	7.50×10^{-3}	3.95×10^{-3}	.577
.325	11.9	1901	8.26×10^{-3}	4.13×10^{-3}	.550
.350	12.0	2070	9.00×10^{-3}	4.33×10^{-3}	.531
.375	12.0	2240	9.74×10^{-3}	4.53×10^{-3}	.515
.400	12.0	2422	.0106	4.61×10^{-3}	.484
.425	12.1	2592	.0113	4.82×10^{-3}	.475
.450	12.1	2786	.0122	4.90×10^{-3}	.450
.475	12.1	2955	.0130	5.06×10^{-3}	.439
.500	12.1	3137	.0137	5.24×10^{-3}	.431
.600	12.2	3885	.0170	5.61×10^{-3}	.375
.700	12.3	4662	.0206	5.76×10^{-3}	.323
.800	12.4	5412	.0240	6.01×10^{-3}	.292
		25.0 milliliters H_2O blank			
.0025		19.8	9.99×10^{-5}		
.0050		39.7	2.00×10^{-4}		
.0075		60.4	2.99×10^{-4}		
.010		81.0	3.98×10^{-4}		
.020		168.1	7.94×10^{-4}		
.030		255.9	1.19×10^{-3}		
.040		340.7	1.58×10^{-3}		
.050		425.9	1.96×10^{-3}		
.100		885.2	3.91×10^{-3}		
.150		1346	5.86×10^{-3}		
.200		1801	7.80×10^{-3}		
.250		2232	9.73×10^{-3}		
.300		2676	.0116		
.352		3111	.0136		
.400		3535	.0155		
.450		3969	.0174		
.500		4389	.0193		
.600		5248	.0230		
.700		6060	.0268		
.800		6851	.0305		

[1]Aqueous NaOH concentrations were determined by the comparison of sample conductivity with that of the blank.

[2]Calculated as the difference between total NaOH added in concentration units and aqueous NaOH concentration.

[3]Calculated using geometric mean of Debye-Huckel activity coefficients for Na^+ and OH^-.

of 1.06×10^{-5} eq/m^2 (1 charge/16 Å^2 of surface or 6.4 sites/nm^2) which is very near to Bowden, Posner, and Quirk's (1977) theoretical limit 10^{-5} eq/m^2 (or 0.965 C m^{-2}). It is also similar in value to the 5 sites/nm^2 for the SiO_2/KCl system attributed by Davis, James, and Leckie (1978) to Armistead and others (1969).

Determination of pH_{pzc}

In order to obtain a thorough perspective of surface characteristics of oxides and silicates, it is common practice to titrate portions of the adsorbent with acid and base at various ionic strengths. The titration curves are then compared with those of blanks containing no adsorbent in order to determine the magnitude of interaction of potential-determining H^+ and OH^- ions as a function of pH at each ionic strength.

The actual quantity measured by such a titration is the net difference ($\Gamma_{H^+}-\Gamma_{OH^-}$) in the adsorption densities of H^+ and OH^- (and hence the surface charge density σ_s); where this equals zero establishes by definition the pH_{pzc}, the pH at which there exists zero surface charge due to the potential-determining ions. The equilibrium constants $K^{ads}_{OH^-}$ and $K^{ads}_{H^+}$ can be determined from such titration data given the "point of zero charge" or pH_{pzc}.

On the basis of the results of the CEC determination, adsorbent with exactly 1.00×10^{-4} equivalent of cation exchange capacity (0.292 gram) was placed in each of two 25.0 mL CO_2-free $NaClO_4$ solutions of 0.001 *M*, two of 0.01 *M*, and two of 0.10 *M*. The adsorbent had been repeatedly rewashed and centrifuged to constant conductivity. The suspensions were then titrated with 1.00 *N* sodium hydroxide and 1.00 *N* perchloric acid.

Between successive additions of acid or base in these six titrations, 3 minutes were allowed for the pH reading to approach equilibrium as the slurry was stirred magnetically. The data for the titrations of these slurries, and for the six blanks of 0.001, 0.01 or 0.10 *M* $NaClO_4$ are shown in table 2.

The method of calculating the surface charge densities is shown in figure 9 for the titration data obtained at 0.001 *M* ionic strength, and the results are plotted in figure 10. The net number of equivalents of charge adsorbed (positive for predominantly H^+ adsorption and negative for predominantly OH^- adsorption) is calculated by the difference between the slurry and the blank in equivalents of acid or base required to attain a given pH. This value is at each titration point divided by the surface area of adsorbent in the slurry (which here is 0.292 g×72.2 m^2/g=21.1 m^2) in order to give the net difference in adsorption density, $\Gamma_{H^+}-\Gamma_{OH^-}$, also listed in table 2. Finally, the surface charge densities are obtained by multiplying these values by the Faraday constant,

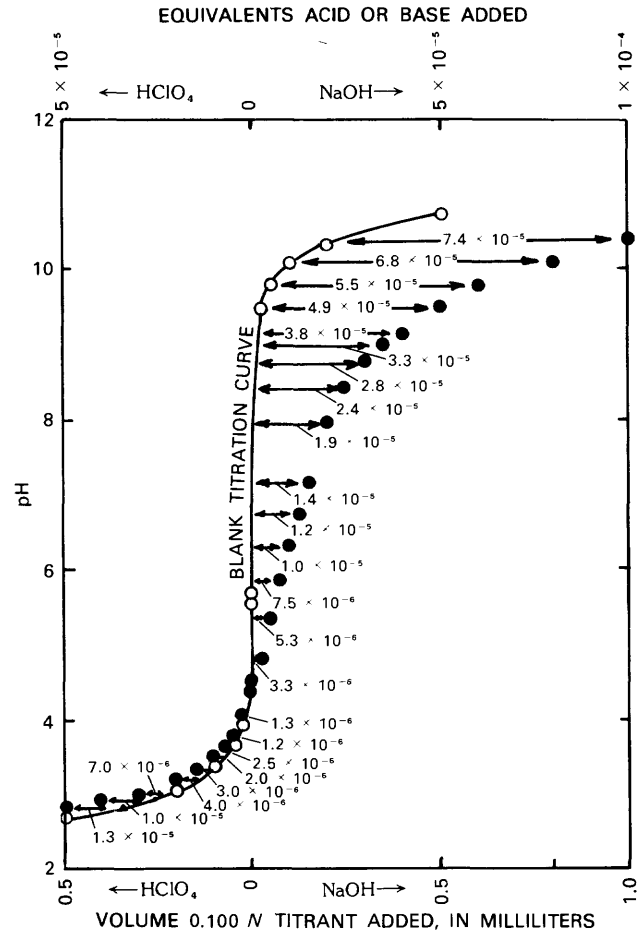

Figure 9. Determination of H^+ and OH^- adsorption by difference between slurry and blank titration data at 0.001 *M* ionic strength for silt fraction of Colma Creek sediment. (Numbers are differences between the two titration curves in equivalents. The pH_{pzc} is the pH at which slurry and blank tritation curves intersect.)

96490 coulombs per equivalent. It can be seen from inspection of the data in table 2 (and from fig. 9 for 0.001 *M* ionic strength) that the surface charge density, at least with respect to H^+ and OH^- ions, becomes zero at the following values of pH, where the adsorbed H^+ ion density Γ_{H^+} is equal to that of OH^-, Γ_{OH^-} :

$NaClO_4$ *Ionic Strength*	pH at which $\Gamma_{H^+}=\Gamma_{OH^-}$
0.0010 *M*	4.3
.010 *M*	4.0
.10 *M*	3.7

Table 2. Titration of adsorbent slurries with 0.100 *N* $HClO_4$ and NaOH

0.292 gram adsorbent in 25 milliliters					*25 milliliters blank*	
Volume (milliliters) of 0.100 N $HClO_4$ or NaOH added	pH	*Equivalents difference from blank*	*($\Gamma_{H^+}-\Gamma_{OH^-}$) Net adsorption density*	*σ_S Surface charge density (Coulombs per square meter)*	*Volume (milliliters) of 0.100 N $HClO_4$ or NaOH added*	pH
Ionic strength=0.001 *M*						
$HClO_4$ added:						
0.000	4.53	-1.0×10^{-6}	-4.7×10^{-8}	−0.0046	0.000	5.69
.025	4.08	1.3×10^{-6}	6.2×10^{-8}	.0059	.025	3.94
.050	3.81	1.2×10^{-6}	5.7×10^{-8}	.0055	.050	3.70
.075	3.67	2.5×10^{-6}	1.2×10^{-7}	.011		
.100	3.50	2.0×10^{-6}	9.5×10^{-8}	.0092	.100	3.43
.150	3.33	3.0×10^{-6}	1.4×10^{-7}	.014		
.200	3.19	4.0×10^{-6}	1.9×10^{-7}	.018	.200	3.08
.300	3.01	7.0×10^{-6}	3.3×10^{-7}	.032		
.400	2.91	1.0×10^{-5}	4.7×10^{-7}	.046		
.500	2.82	1.3×10^{-5}	6.2×10^{-7}	.010	.500	2.75
NaOH added:						
0.000	4.40	-1.0×10^{-6}	-4.7×10^{-8}	−0.0046	0.000	5.53
.025	4.80	-3.3×10^{-6}	-1.6×10^{-7}	−.015	.025	9.46
.050	5.36	-5.3×10^{-6}	-2.5×10^{-7}	−.024	.050	9.76
.075	5.85	-7.5×10^{-6}	-3.6×10^{-7}	−.034		
.100	6.31	-1.0×10^{-5}	-4.7×10^{-7}	−.046	.100	10.06
.125	6.73	-1.2×10^{-5}	-5.7×10^{-7}	−.055		
.150	7.15	-1.4×10^{-5}	-6.6×10^{-7}	−.064		
.200	7.95	-1.9×10^{-5}	-9.0×10^{-7}	−.087	.200	10.29
.250	8.42	-2.4×10^{-5}	-1.1×10^{-6}	−.110		
.300	8.76	-2.8×10^{-5}	-1.3×10^{-6}	−.128		
.350	8.98	-3.3×10^{-5}	-1.6×10^{-6}	−.151		
.400	9.14	-3.8×10^{-5}	-1.8×10^{-6}	−.174		
.500	9.50	-4.9×10^{-5}	-2.3×10^{-6}	−.215	.500	10.72
.600	9.77	-5.5×10^{-5}	-2.6×10^{-6}	−.252		
.800	10.13	-6.8×10^{-5}	-3.2×10^{-6}	−.311		
1.000	10.35	-7.4×10^{-5}	-3.5×10^{-6}	−.339	1.000	11.04
1.500	10.72	-1.00×10^{-4}	-4.7×10^{-6}	−.458		
2.000	10.91	-1.23×10^{-4}	-5.8×10^{-6}	−.563	2.000	11.33
5.000	11.40	-2.30×10^{-4}	-1.09×10^{-5}	−1.053	5.000	11.60
Ionic strength=0.01 *M*						
$HClO_4$ added:						
0.000	4.34	-2.8×10^{-6}	-1.3×10^{-7}	−0.013	0.000	5.42
.025	3.97	0	0	0	.025	3.96
.050	3.81	2.0×10^{-6}	9.5×10^{-8}	0.009	.050	3.68
.075	3.65	2.0×10^{-6}	9.5×10^{-8}	.009		
.100	3.47	2.7×10^{-6}	8.1×10^{-8}	.008	.100	3.40
.150	3.34	3.0×10^{-6}	1.4×10^{-7}	.014		
.200	3.20	4.0×10^{-6}	1.9×10^{-7}	.018	.200	3.08
.300	3.01	4.5×10^{-6}	2.1×10^{-7}	.021		
.400	2.88	6.5×10^{-6}	3.1×10^{-7}	.030		
.500	2.81	8.5×10^{-6}	4.0×10^{-7}	.039	.500	2.75

Table 2. Titration of adsorbent slurries with 0.100 *N* $HClO_4$ and NaOH—Continued

0.292 gram adsorbent in 25 milliliters					*25 milliliters blank*	
Volume (milliliters) of 0.100 N $HClO_4$ or NaOH added	pH	*Equivalents difference from blank*	$(\Gamma_{H^+} - \Gamma_{OH^-})$ *Net adsorption density*	σ_s *Surface charge density (Coulombs per square meter)*	*Volume (milliliters) of 0.100 N $HClO_4$ or NaOH added*	pH
Ionic strength=0.01 *M*—Continued						
NaOH added:						
0.000	4.20	-2.0×10^{-6}	-9.5×10^{-8}	−0.009	0.000	5.68
.025	4.45	-3.5×10^{-6}	-1.7×10^{-7}	−.016	.025	9.65
.050	4.82	-5.5×10^{-6}	-2.6×10^{-7}	−.025	.050	10.01
.075	5.32	-7.5×10^{-6}	-3.6×10^{-7}	−.034		
.100	5.81	-9.5×10^{-6}	-4.5×10^{-7}	−.043	.100	10.35
.125	6.36	-1.2×10^{-5}	-5.7×10^{-7}	−.055		
.150	6.70	-1.4×10^{-5}	-6.6×10^{-7}	−.064		
.200	7.45	-2.0×10^{-5}	-0.5×10^{-7}	−.092	.200	10.57
.250	8.01	-2.4×10^{-5}	-1.1×10^{-6}	−.110		
.300	8.43	-2.9×10^{-5}	-1.4×10^{-6}	−.133		
.350	8.76	-3.4×10^{-5}	-1.6×10^{-6}	−.156		
.400	9.05	-3.8×10^{-5}	-1.8×10^{-6}	−.174		
.500	9.49	-4.8×10^{-5}	-2.3×10^{-6}	−.220	.500	10.95
.600	9.78	-5.2×10^{-5}	-2.5×10^{-6}	−.238		
.800	10.17	-7.3×10^{-5}	-3.5×10^{-6}	−.334		
1.000	10.43	-8.7×10^{-5}	-4.1×10^{-6}	−.398	1.000	11.22
1.500	10.83	-1.12×10^{-4}	-5.3×10^{-6}	−.513		
2.000	11.16	-1.20×10^{-4}	-5.69×10^{-6}	−.549	2.000	11.45
5.000	11.46	-3.00×10^{-4}	-1.42×10^{-5}	−1.37	5.000	11.69
Ionic strength=0.10 *M*						
0.000	4.08	-2.0×10^{-6}	-9.5×10^{-8}	−0.009	0.000	4.70
.025	3.86	-1.0×10^{-6}	-4.7×10^{-8}	−.005	.025	3.98
.050	3.66	0	0	0	.050	3.71
.075	3.53	1.0×10^{-6}	4.7×10^{-8}	.005		
.100	3.43	1.0×10^{-6}	4.7×10^{-8}	.005	.100	3.42
.150	3.26	1.0×10^{-6}	4.7×10^{-8}	.005		
.200	3.12	1.0×10^{-6}	4.7×10^{-8}	.005	.200	3.09
.300	2.95	2.0×10^{-6}	9.5×10^{-8}	.009		
.400	2.82	2.5×10^{-6}	1.2×10^{-7}	.001		
.500	2.72	4.8×10^{-6}	2.3×10^{-7}	.022	.500	2.72

Table 2. Titration of adsorbent slurries with 0.100 *N* $HClO_4$ and NaOH—Continued

0.292 gram adsorbent in 25 milliliters					*25 milliliters blank*	
Volume (milliliters) of 0.100 N $HClO_4$ or NaOH added	pH	*Equivalents difference from blank*	$(\Gamma_{H^+} - \Gamma_{OH^-})$ *Net adsorption density*	σ_s *Surface charge density (Coulombs per square meter)*	*Volume (milliliters) of 0.100 N $HClO_4$ or NaOH added*	pH
Ionic strength = 0.10 *M*—Continued						
NaOH added:						
0.000	4.04	-2.0×10^{-6}	-9.5×10^{-8}	−0.009	0.000	4.61
.025	4.34	-3.0×10^{-6}	-1.4×10^{-7}	−.014	.025	9.32
.050	4.69	-5.0×10^{-6}	-2.4×10^{-7}	−.023	.050	9.82
.075	5.17	-7.5×10^{-6}	-3.6×10^{-7}	−.034		
.100	5.68	-9.5×10^{-6}	-4.5×10^{-7}	−.043		
.125	6.15	-1.15×10^{-5}	-5.5×10^{-7}	−.053		
.150	6.51	-1.4×10^{-5}	-6.6×10^{-7}	−.064		
.200	7.18	-1.9×10^{-5}	-9.0×10^{-7}	−.087		
.250	7.73	-2.35×10^{-5}	-1.11×10^{-6}	−.108		
.300	8.09	-2.85×10^{-5}	-1.35×10^{-6}	−.130		
.350	8.43	-3.3×10^{-5}	-1.6×10^{-6}	−.151		
.400	8.75	-3.8×10^{-5}	-1.8×10^{-6}	−.174		
.500	9.28	-4.8×10^{-5}	-2.3×10^{-6}	−.220		
.600	9.60	-5.65×10^{-5}	-2.68×10^{-6}	−.259		
.800	10.07	-7.3×10^{-5}	-3.5×10^{-6}	−.334		
1.000	10.37	-8.6×10^{-5}	-4.1×10^{-6}	−.394		
2.000	11.00	-1.20×10^{-4}	-5.7×10^{-6}	−.594		
5.000	11.38	-2.49×10^{-4}	-1.18×10^{-5}	−1.14		

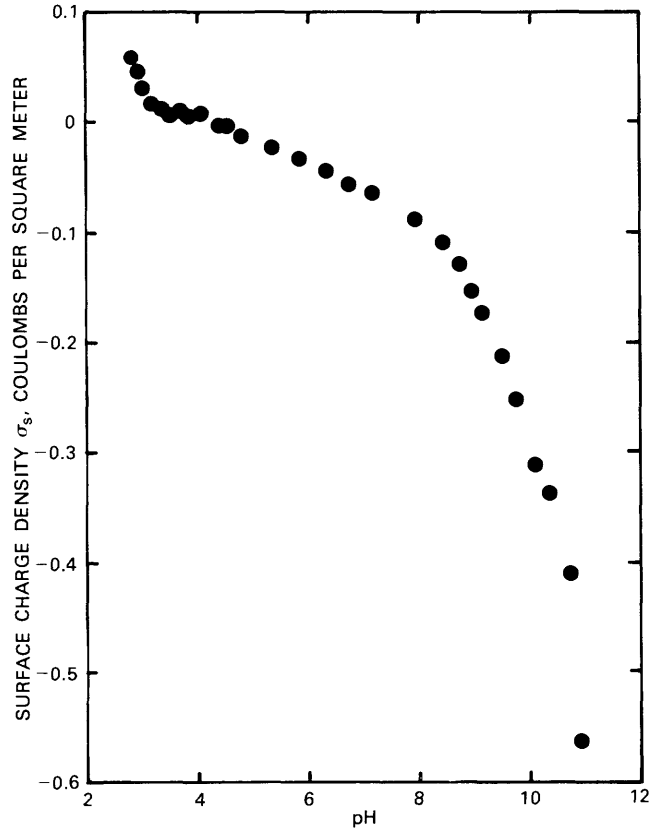

Figure 10. Density of surface charge on silt fraction of Colma Creek sediment as a function of pH at 0.001 *M* ionic strength.

Depending on which terminology convention is used, a pH value at a given background electrolyte concentration is called the point-of-zero-charge-pH (pH_{pzc}) or isoelectric point (IEP)[2], the latter referring to a pH at which the adsorption densities Γ_{H^+} and Γ_{OH^-} of the potential-determining ions H^+ and OH^- are equal, and pH_{pzc} (or PZC) referring to a net zero surface charge when all specifically adsorbing ions are taken into account, as noted by Bowden, Posner, and Quirk (1977). The above-measured pH values are the IEP values at individual ionic strengths. Normally, in the presence of an "inert" (non-adsorbing) electrolyte, such measured IEP values should be independent of electrolyte concentration; plots of surface charge density σ_s (or $N_s F(\Gamma_{H^+} - \Gamma_{OH^-})$) as a function of pH at different ionic strengths should cross the zero axis at the same pH. (In the limiting case, the IEP and the pH_{pzc} would be equal.) The plot will not cross the zero axis at the same pH, however, when the electrolyte is not quite "inert," and its cations or anions do adsorb; the measured IEP value will depend on electrolyte concentration, and the IEP will approach the pH_{pzc} as the ionic strength approaches zero. Since it is not clear exactly how the IEP relates to the PZC as a function of ionic strength, we will use for our pH_{pzc} simply the value obtained at the lowest ionic strength (0.001 *M*)—4.3. For the purpose of attempting to reconcile theory with experiment, this value is probably appropriate because our experimental work was performed at an ionic strength which hovers about 10^{-3} *M*, as does the ionic strength of many natural waters.

[2]The respective meanings of pH_{pzc} (or PZC) and IEP have been confusingly switched back and forth over the years.

Determination of $K_{H^+}^{ads}$

In order to deduce a method by which we might extract $K_{H^+}^{ads}$ or $K_{OH^-}^{ads}$ from the preceding experimental data, we first write the Langmuir adsorption expression for H^+ ion:

$$\Gamma_{H^+} = \frac{N_s K_{H^+}^{ads} [H^+] e^{-F\psi_s/RT}}{1 + K_{H^+}^{ads} [H^+] e^{-F\psi_s/RT} + K_{OH^-}^{ads} [OH^-] e^{+F\psi_s/RT}} . \quad (64)$$

One approximation (which can be used only for data where both Γ_{H^+} and Γ_{OH^-} are small relative to N_s and the pH does not depart significantly from the pH_{pzc}) is that $|\psi_s|$ is small, perhaps less than 25 mV. As a result, the exponential terms in the denominator of equation 64 will approach unity; at values of pH near the pH_{pzc}, the terms in the denominator will also be much smaller than the second and third one. Equation 64 will then become

$$\Gamma_{H^+} \approx N_s K_{H^+}^{ads} [H^+] e^{-F\psi_s/RT} \quad (66)$$

Atkinson, Posner, and Quirk (1967) have shown that as a consequence of the smallness of $|\psi_s|$, the term $F\psi_s/RT$ is approximately given by

$$\frac{F\psi_s}{RT} \approx \sigma_s \sqrt{\frac{1}{2000 \epsilon_0 \epsilon_{H_2O} RT\mu}} \quad (67)$$

Since $\sigma_s = F(\Gamma_{H^+} - \Gamma_{OH^-})$, this becomes

$$\frac{F\psi_s}{RT} \approx F(\Gamma_{H^+} - \Gamma_{OH^-}) \sqrt{\frac{1}{2000 \epsilon_0 \epsilon_{H_2O} RT\mu}} . \quad (68)$$

Substituting equation 68 into equation 66, taking logarithms, and rearranging, we obtain

$$\log_{10}\Gamma_{H^+} + pH \approx \log_{10} K^{ads}_{H^+} N_s - \frac{F(\Gamma_{H^+} - \Gamma_{OH^-})}{2.303}\sqrt{\frac{1}{2000\epsilon_0\epsilon_{H_2O}RT\mu}} \quad (69)$$

Thus, a plot of the sum of pH and $\log_{10}(\Gamma_{H^+} - \Gamma_{OH^-})$ —which is approximately equal to $\log_{10}\Gamma_{H^+}$ when Γ_{OH^-} is negligible—as a function of $(\Gamma_{H^+} - \Gamma_{OH^-})$ should give an intercept of $\log_{10} K^{ads}_{H^+} N_s$, within the limits of the assumptions and approximations used for deriving the above expression. These approximations potentially present somewhat of a problem because we have assumed (1) that Γ_{OH^-} is negligible in relation to Γ_{H^+}, an assumption that begins to break down as the pH approaches the pH_{pzc}, and (2) that Γ_{H^+} and Γ_{OH^-} are both quite low and $|\psi_s|$ is small; this occurs at pH values only slightly lower than the pH_{pzc}, and the assumption breaks down as the pH is decreased below the pH_{pzc}. A plot of $\log_{10}(\Gamma_{H^+} - \Gamma_{OH^-}) + pH$ versus $(\Gamma_{H^+} - \Gamma_{OH^-})$ will, therefore, deviate from linearity at very large and very small values of $(\Gamma_{H^+} - \Gamma_{OH^-})$—there existing between these two extremes a group of data points which exhibit linear behavior.

It can be shown by means of a similar analysis of the OH^- ion that the Langmuir expression,

$$\Gamma_{OH^-} = \frac{N_s K^{ads}_{OH^-}[OH^-]e^{+F\psi_s/RT}}{1 + K^{ads}_{H^+}[H^+]e^{-F\psi_s/RT} + K^{ads}_{OH^-}[OH^-]e^{+F\psi_s/RT}}, \quad (70)$$

can be simplified to an expression analogous to equation 66, namely:

$$\Gamma_{OH^-} \approx N_s K^{ads}_{OH^-}[OH^-]e^{+F\psi_s/RT} \quad (71)$$

This will be true if we utilize the approximation that both Γ_{H^+} and Γ_{OH^-} are quite low and $|\psi_s|$ is small, and will be less valid as the pH is increased above the pH_{pzc}. Taking logarithms and rearranging, this becomes

$$\log_{10}\Gamma_{OH^-} - \log_{10}[OH^-] \approx \log_{10}(K^{ads}_{OH^-} N_s) + \frac{F\psi_s}{2.303RT}. \quad (72)$$

Substitution of equation 68 into equation 72 yields

$$\log_{10}\Gamma_{OH^-} - \log_{10}[OH^-] \approx \log_{10}(K^{ads}_{OH^-} N_s) + \frac{F(\Gamma_{H^+} - \Gamma_{OH^-})}{2.303}\sqrt{\frac{1}{2000\epsilon_0\epsilon_{H_2O}RT\mu}}. \quad (73)$$

From equation 43 we have

$$K^{ads}_{H^+}[H^+_{pzc}] = K^{ads}_{OH^-}[OH^-_{pzc}], \quad (43)$$

where $[H^+_{pzc}]$ and $[OH^-_{pzc}]$ are the respective aqueous H^+ and OH^- activities at a pH equal to the pH_{pzc}. Since equilibrium requires that $[OH^-_{pzc}] = K_w/[H^+_{pzc}]$, substitution and rearrangement of equation 43 yields

$$K^{ads}_{OH^-} = \frac{K^{ads}_{H^+}[H^+_{pzc}]^2}{K_w}. \quad (74)$$

Water dissociation equilibrium will also dictate at any pH that $\log_{10}[OH^-] = \log_{10}K_w + pH$. Substitution of this relationship and that of equation 74 into equation 73 will yield, after some rearrangement

$$\log_{10}\Gamma_{OH^-} - pH + 2pH_{pzc} = \log_{10}(K^{ads}_{H^+} N_s) + \frac{F(\Gamma_{H^+} - \Gamma_{OH^-})}{2.303}\sqrt{\frac{1}{2000\epsilon_0\epsilon_{H_2O}RT\mu}}. \quad (75)$$

Within the limits in which Γ_{H^+} is negligible in relation to Γ_{OH^-} {where $pH > pH_{pzc}$ so that $\Gamma_{OH^-} \approx -(\Gamma_{H^+} - \Gamma_{OH^-})$} a plot of $\log_{10}[-(\Gamma_{H^+} - \Gamma_{OH^-})] - pH + 2pH_{pzc}$ as a function of $(\Gamma_{OH^-} - \Gamma_{H^+})$ should yield an intercept equal to $\log_{10}(K^{ads}_{H^+} N_s)$. Similarly, and as indicated by equation 69, a plot of $\log_{10}(\Gamma_{H^+} - \Gamma_{OH^-}) + pH$ as a function of $(\Gamma_{H^+} - \Gamma_{OH^-})$, should for $pH < pH_{pzc}$, also yield the same intercept. Titration data to be used for this purpose are given in table 3 and are plotted in figure 11.

Table 3. Adsorbent titration data for use in calculating $\log_{10} K_{H^+}^{ads} N_s$

pH	$\Gamma_{H^+} - \Gamma_{OH^-}$ (equivalents per square meter)	$\log_{10}[(\Gamma_{H^+} - \Gamma_{OH^-})] + pH$	$\log_{10}[(\Gamma_{H^+} - \Gamma_{OH^-})] - pH + 2pH_{pzc}$	
	Ionic strength = 0.001 *M* (pH_{pzc} = 4.3)			
2.82	6.2×10^{-7}	−3.39		
2.91	4.7×10^{-7}	−3.42		
3.01	3.3×10^{-7}	−3.47		
3.19	1.9×10^{-7}	−3.53		
3.33	1.4×10^{-7}	−3.52		
3.50	9.5×10^{-8}	−3.52		
3.67	1.2×10^{-7}	−3.25		
3.81	5.7×10^{-8}	−3.43		
4.08	6.2×10^{-8}	−3.13		
4.40	-4.7×10^{-8}		−3.13	
4.53	-4.7×10^{-8}		−3.26	
4.80	-1.6×10^{-7}		−3.00	┐
5.36	-2.5×10^{-7}		−3.36	│ These points lie
5.85	-3.6×10^{-7}		−3.69	│ in a straight line
6.31	-4.7×10^{-7}		−4.04	│ with intercept
6.73	-5.7×10^{-7}		−4.37	│ −2.52
7.15	-6.6×10^{-7}		−4.73	┘
7.95	-9.0×10^{-7}		−5.40	
8.42	-1.1×10^{-6}		−5.78	
8.76	-1.3×10^{-6}		−6.05	
8.98	-1.6×10^{-6}		−6.18	
9.14	-1.8×10^{-6}		−6.28	
9.50	-2.3×10^{-6}		−6.54	
9.77	-2.6×10^{-6}		−6.76	
10.13	-3.2×10^{-6}		−7.02	
10.35	-3.5×10^{-6}		−7.21	
10.72	-4.7×10^{-6}		−7.45	
10.91	-5.8×10^{-6}		−7.55	
11.40	-1.09×10^{-5}		−7.76	
	Ionic strength = 0.010 *M* (pH_{pzc} = 4.0)			
2.81	4.0×10^{-7}	−3.59		
2.88	3.1×10^{-7}	−3.63		
3.01	2.1×10^{-7}	−3.67		
3.20	1.9×10^{-7}	−3.52		
3.34	1.4×10^{-7}	−3.51		
3.47	8.1×10^{-8}	−3.62		
3.65	9.5×10^{-8}	−3.37		
3.81	9.5×10^{-8}	−3.21		
3.97	0			
4.20	-9.5×10^{-8}		−3.22	
4.34	-1.3×10^{-7}		−3.23	
4.45	-1.7×10^{-7}		−3.22	
4.82	-2.6×10^{-7}		−3.41	┐
5.32	-3.6×10^{-7}		−3.76	│ These points lie
5.81	-4.5×10^{-7}		−4.15	│ in a straight line
6.36	-5.7×10^{-7}		−4.60	│ with intercept
6.70	-6.6×10^{-7}		−4.88	┘ −2.47

Table 3. Adsorbent titration data for use in calculating $\log_{10} K_{H^+}^{ads} N_s$—Continued

pH	$\Gamma_{H^+} - \Gamma_{OH}$ (equivalents per square meter)	$\log_{10}([\Gamma_{H^+} - \Gamma_{OH^-}]) + pH$	$\log_{10}[(\Gamma_{H^+} - \Gamma_{OH^-})] - pH + 2pH_{pzc}$	
	Ionic strength = 0.010 *M* (pH_{pzc} = 4.0)—Continued			
7.45	-9.5×10^{-7}		−5.47	
8.01	-1.1×10^{-6}		−5.97	
8.43	-1.4×10^{-6}		−6.28	
8.76	-1.6×10^{-6}		−6.56	
9.05	-1.8×10^{-6}		−6.79	
9.49	-2.3×10^{-6}		−7.13	
9.78	-2.5×10^{-6}		−7.38	
10.17	-3.5×10^{-6}		−7.63	
10.43	-4.1×10^{-6}		−7.82	
10.83	-5.31×10^{-6}		−8.10	
11.16	-5.69×10^{-6}		−8.40	
11.46	-1.42×10^{-5}		−8.31	
	Ionic strength = 0.10 *M* (pH_{pzc} = 3.7)			
2.72	2.3×10^{-7}	−3.92		
2.82	1.2×10^{-7}	−4.10		
2.95	9.5×10^{-8}	−4.07		
3.12	4.7×10^{-8}	−4.21		
3.26	4.7×10^{-8}	−4.07		
3.43	4.7×10^{-8}	−3.90		
3.53	4.7×10^{-8}	−3.80		
3.66	0			
3.86	-4.7×10^{-8}		−3.79	
4.04	-9.5×10^{-8}		−3.66	
4.08	-9.5×10^{-8}		−3.70	
4.34	-1.4×10^{-7}		−3.79	
4.69	-2.4×10^{-7}		−3.91	These points lie
5.17	-3.6×10^{-7}		−4.21	in a straight line
5.68	-4.5×10^{-7}		−4.63	with intercept
6.15	-5.5×10^{-7}		−5.01	−3.38
6.51	-6.6×10^{-7}		−5.29	
7.18	-9.0×10^{-7}		−5.83	
7.73	-1.11×10^{-6}		−6.28	
8.09	-1.35×10^{-6}		−6.56	
8.43	-1.6×10^{-6}		−6.83	
8.75	-1.8×10^{-6}		−7.09	
9.28	-2.3×10^{-6}		−7.52	
9.60	-2.68×10^{-6}		−7.77	
10.07	-3.5×10^{-6}		−8.13	
10.37	-4.1×10^{-6}		−8.36	
11.00	-5.7×10^{-6}		−8.84	
11.38	-1.18×10^{-5}		−8.91	

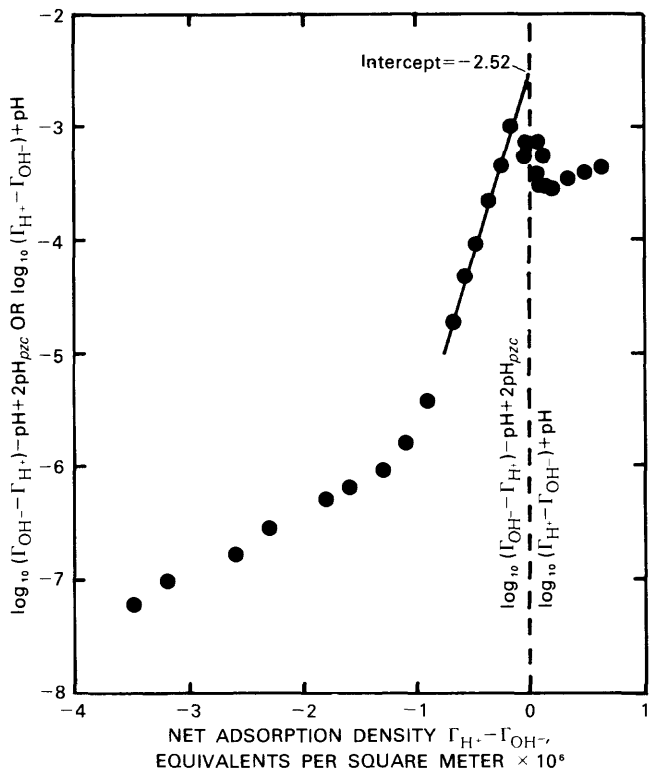

Figure 11. Linear extrapolation of adsorbent titration data for determination of $\log_{10}K_{ads}N_s$ at 0.001 *M* ionic strength.

Figure 11 illustrates, for ionic strength 0.001 *M*, how the sets of data points at which there is greater OH^- than H^+ adsorption (left or ordinate) and vice versa (right or ordinate) tend to converge near the same intercepts as $(\Gamma_{H^+}-\Gamma_{OH^-})$ approaches zero. The points to the left, however, show this more clearly because there is more data for which the pH is greater than the pH_{pzc} than for which it is less. The intercepts approached from the left side involve data for which the pH is greater than 4 and are much more relevant in terms of natural water pH than is our data for pH less than 4. It can be seen from data in table 3 (and from fig. 11 for 0.001 *M* ionic strength) that the intercepts drawn through the straight line data points give intercepts equal to $\log_{10}(K^{ads}_{H^+}N_s)$, as follows:

Ionic Strength	$\log_{10}(K^{ads}_{H^+}N_s)$
0.0010 *M*	−2.52
.010 *M*	−2.47
.10 *M*	−3.38

While the values of the intercept at the two lower ionic strengths are very nearly equal, the value of −3.38 at the high ionic strength of 0.10 *M* departs drastically from those of the lower ionic strengths. This may be an indication that the sodium perchlorate electrolyte interacts with the adsorbent in a manner for which we have not yet theoretically accounted. For example, specific adsorption of electrolyte ions may become appreciable near 0.10 *M* concentration. In any case, we are not concerned at this time with adsorption in solutions of such high ionic strength. We will, therefore, utilize for the intercept the value of −2.52 obtained at the lowest ionic strength.

The intercept, of course, is equal to $\log_{10}K^{ads}_{H^+}N_s$, where $K^{ads}_{H^+}N_s$ has units of liters per square meter. Since N_s was earlier found to be 1.06×10^{-5} mol m^{-2}, a value for $K^{ads}_{H^+}N_s$, of $10^{-2.52}$ (at 0.001 *M* ionic strength) requires that $K^{ads}_{H^+}$ equal $10^{2.45}$. Given the pH_{pzc} of 4.3, equation 45 dictates that K^{ads} equal $10^{7.85}$, more than five orders of magnitude larger than $K^{ads}_{H^+}$.

Dielectric Constant

The value of the dielectric constant ϵ_{solid} of the adsorbing solid is important in determining the magnitude of the change in free energy of solvation of the adsorbed ion. This term is used in both the James-Healy and Levine (1971) expressions for the solvation free energy term, and figure 2 illustrates the dramatic effect of the ϵ_{solid} value on the calculated value for ΔG^{solv}. Consequently, the dielectric constant of the solid is extremely important in determining the relative values of $\Delta G^{solv}_{Pb^{+2}}$ and $\Delta G^{solv}_{PbOH^+}$, and hence the relative proportions of Pb^{+2} and $PbOH^+$ adsorption. The usual method for measuring the dielectric constant of a solid is to grind a sample into a thin flat plate for use as a dielectric between two capacitor plates. The dielectric constant is equal to the ratio of the capacitance attributable to the plate, as measured by an ac capacitance bridge, to the capacitance for the same assembly with only air between the plates. This method presents several difficulties when one attempts to adapt it for the determination of the dielectric constant of powdered substances. First, the powder must be placed in a matrix of polystyrene or other solidifying liquid. (Sometimes air is used as the medium and the powder is compressed to form a plate.) Second, there is no firmly established universal formula for mathematically extracting the dielectric constant of the solid component of interest from the overall dielectric constant for the pressed or solidified mixture. Approaches to this problem depend in part on the value of the solid dielectric constant itself and were discussed at length by Yadav and Parshad (1972) and Lal and Parshad (1974). The overall dielectric constant is not a simple function of the volume fractions and dielectric constants of the mixture components.

In order to determine the capacitance of a cell containing the powdered adsorbent, such a cell was

fashioned from phenolic copper-clad boards 6 cm square, placed about 1mm apart, and glued at the edges with epoxy glue. A cell calibration curve was prepared by capacitance bridge measurement for liquids of various known dielectric constants which were placed in the cell, and the cell volume was found to be 2.714 cm^3. The cell was then filled with 1.131 g of adsorbent, and the capacitance was measured while vigorously shaking; in one case air was used as the dispersion medium, and in another case, cyclohexane, which was used because of its low electrical loss properties. The adsorbent's density was found to be 2.409 g/cm^3 by determining the density of a chloroform-bromoform mixture in which the adsorbent particles would barely begin to float as more bromoform was added. The volume of adsorbent in both instances then was 0.469 cm^3, yielding a volume fraction in the cell of 0.173.

The cell capacitances were measured with a 1,000-Hz ac capacitance bridge while the cell was being vigorously shaken so to keep the particles suspended in air and in cyclohexane; the values of capacitance measured were, respectively, 100.5 and 127.7 picofarads. These values correspond to respective overall mixture dielectric constants of 1.942 and 3.267, according to the cell calibration data which are presented in table 4.

Lal and Parshad (1974) suggested the use of Looyenga's (1965) equation for determining the dielectric constant for solid components in mixtures. This equation, stated to be valid only if it yields solid dielectric constants of greater than 7, can be expressed

$$\epsilon_{solid} = \left[\epsilon_{medium}^{1/3} + \left(\frac{\epsilon_{measured}^{1/3} - \epsilon_{medium}^{1/3}}{V_{solid}}\right)\right]^3 . \quad (76)$$

The terms ϵ_{solid}, ϵ_{medium}, and $\epsilon_{measured}$ are the respective dielectric constants for the solid particles of interest, the dispersing medium, and the measured experimental value of the mixture; the V_{solid} term refers to the volume fraction of the solid of interest. Using our value of V_{solid} (0.173) and the measured dielectric constants of 1.942 for the air suspension ($\epsilon_{medium} = 1.000$) and 3.267 for the cyclohexane ($\epsilon_{medium} = 2.015$ at 25°C), we obtain from the above equation respective ϵ_{solid} values of 14.4 (in air) and 16.4 (in cyclohexane). These values are within reasonable agreement with one another, and the fact that they are substantially greater than 7 appears to justify the use of the Looyenga (1965) formula. We shall use the value of 16.4 for the dielectric constant of the solid adsorbent because the powder was probably better

Table 4. Capacitance data used in determining dielectric constant of powdered adsorbent[1]

Material placed in cell[2]	*Capacitance (picofarads)*	*Dielectric constant at 25°C*	*Comments*
		CALIBRATION	
Nothing (air)	81.0	1.000	Least square analysis of calibration data
Cyclohexane	102.8	2.015	leads to relation: capacitance (picofarads)
Carbon tetrachloride	106.0	2.228	= 60.63 + 20.53ϵ (r = 0.999).
Benzene	107.0	2.274	
		DETERMINATION[3]	
1.13094 gram adsorbent in air	100.5	1.942	Looyenga's (1965) formula[4] yields ϵ_{solid} of 14.4.
1.13094 gram adsorbent in cyclohexane	127.7	3.267	Looyenga's (1965) formula[4] yields ϵ_{solid} of 16.4.

[1]Adsorbent density is 2.409 g/cm^3.

[2]Cell volume is 2.714 cm^3 by weight of water held at 25°C.

[3]Dielectric constant determined from rearranged calibration formula ϵ=(capacitance, pF−60.63)/20.53.

[4]1.13094 gram adsorbent, at 2.409 g/cm^3, has volume of 0.469 cm^3 out of 2.714 cm^3 cell volume, so that solid volume fraction V_{solid} equals 0.173 for use in Looyenga's (1965) formula.

suspended and dispersed in the presence of cyclohexane than it was in air. (It is unfortunate, however, that the determination could not have been made in the presence of water due to high dielectric losses resulting from the very polar nature of water.)

It should be noted that the dielectric constant for the bulk particles as measured here may in a strict sense be incorrect in that we extrapolate that value to a hydrated surface environment which has undergone substantial changes in electrical properties (at least with respect to the surface if not the bulk) upon addition of water. (Levine (1971) used the value of 10 for ϵ_{solid} in the ΔG_i^{solv} term for ion adsorption on quartz, despite the fact that the bulk dielectric constant of quartz is 4.3.) We shall, nevertheless, use our experimental value for want of a more rigorous one.

Summary of Adsorbent Properties

The chemical parameters obtained for the adsorbent thus far are as follows:

Cation-exchange capacity	3.42×10^{-4} equivalent per gram
Surface area	$72.2\ m^2/g$
N_s	7.63×10^{-5} eq./g, or 1.06×10^{-5} eq/m^2
pH_{pzc}	4.3
$K_{H^+}^{ads}$	$10^{2.45}$ dm^3/mol
ϵ_{solid}	16.4

ADSORPTION OF LEAD

The usual technique for determining the amount of adsorption of a heavy metal under a given set of conditions is to prepare a solution containing a known concentration of the metal to which is added a known amount of adsorbent. After establishment of chemical equilibrium, the concentration remaining in solution is measured; the decrease in concentration is presumed, in the absence of precipitation, to result from adsorption. The amount adsorbed, when referenced to the volume of the system, can be treated as an adsorbed species concentration which can be used in various equilibrium expressions purporting to describe the system.

The slurries prepared in this manner in our experiments had total aqueous lead concentrations (ΣPb) of 5.0×10^{-4} and 1.0×10^{-4} *M* prior to adsorption. These concentrations, large in comparison to those normally found in natural waters, were used mainly for two reasons:

First, sediments in natural waters usually are at equilibrium with the waters containing moderate concentrations of Na^+, Ca^{+2}, Mg^{+2}, and K^+. The sediment adsorption sites are, therefore, moderately saturated or near-saturated with these species, particularly Ca^{+2} and Mg^{+2}. These adsorbed cations undoubtedly exert mutually perturbing effects on each others' adsorption behavior and on that of the heavy metal cations. (Indeed, the VSC–VSP model takes into account the sum of the charges of all adsorbed cations in altering the surface charge density σ_s and surface potential ψ_s.) For us, however, to attempt at this stage to model thoroughly this effect would require us to consider the simultaneous adsorption of Na^+, Ca^{+2}, Mg^{+2}, and K^+. Although our studies are conducted with this eventual goal in mind, this sort of analysis is beyond the scope of this paper. As an alternative, however, we instead use concentrations of total lead which will give rise to a realistically large adsorption density of adsorbed cations in order that we may determine the magnitude of this type of effect while concerning ourselves with the less complex situation of adsorption of only one metal.

Second, a total lead content which approaches (but does not exceed) the maximum quantity of adsorbed cation that can be accommodated by the adsorbent will give rise to an adsorption "edge" (referring to the rise in percent of total metal adsorbed as function of pH) which will rise gradually with pH rather than suddenly shift from a very low to a very high adsorption, as is characteristic in many studies of adsorption of hydrolzable heavy metals. Adsorption, which increases only gradually as pH is increased, will yield a larger amount of useful data in the important range between two extremes of near-zero and near-total adsorption where experimental uncertainties tend to more greatly affect interpretation of the data. For an adsorption which increases rapidly with pH, all that anyone need do in "fitting", for example, the James-Healy (1972) model to the data is to find the proper values of ΔG_{Pb}^{chem} which will describe the pH at which the sudden increase in adsorption occurs. For a large total lead concentration, however, we will be better able to determine whether the model will properly describe the adsorption edge.

In order to reduce the number of chemical species present and thereby simplify the system, 10 separate portions of adsorbent of 0.146 gram (each equal to 5.0×10^{-5} equivalent at the CEC of 3.42×10^{-4} eq/g were washed to constant conductivity with deionized water in order to remove any adsorbed ions, and were each placed in 50 mL of solution (so that the CEC per unit volume was 1.0×10^{-3} eq/L) which contained either 1.0×10^{-4} or 5.0×10^{-4} *M* lead perchlorate in CO_2-free deionized distilled water. The pH was then adjusted, by the addition of 1.0 *N* sodium hydroxide or 1.0 *N* perchloric acid as appropriate, to values of approximately 2, 3, 4, 5, and 6 for both the 5.0×10^{-4} and 1.0×10^{-4} *M* sets of solutions. These slurries were then placed in a CO_2-free atmosphere

at 25°C for 48 hours, in order to assure a close approach to equilibrium, during which time the slurries were magnetically stirred for 5 minutes every half hour.

After 48 hours, the slurries were removed from the CO_2-free atmosphere, and the pH was measured. Aliquots of 5 mL were then removed and centrifuged at 30,000 *G*'s for 5 minutes in order to remove any suspended particulate matter. The centrifuged solutions were then analyzed for lead and sodium by atomic absorption spectrophotometry, for which the data are shown in table 5. It can be seen from this data in table 5, particularly for the 5.0×10^{-4} *M* Pb slurries, that the rate of increase of percent adsorption with pH is quite gradual. Even the 1.0×10^{-4} *M* adsorption data showed an adsorption rise which, although more rapid than the 5.0×10^{-4} *M* data, is still much more gradual than that which would be predicted using the model of James and Healy (1972). It should be noted at this point that the calculated Pb^{+2} and OH^- activities of all solutions indicated that the lead solubility was not controlled by $Pb(OH)_2$ precipitation, but rather by adsorption. All $[Pb^{+2}]\ [OH^-]^2$ activity products were smaller than the $Pb(OH)_2$ solubility product of $10^{-19.84}$. Since the value of the "chemical" free energy term is normally found by determining the value which best fits experimental adsorption to theoretical adsorption based on the experimental pH values, a computer program was designed which would select the best James-Healy ΔG_{Pb}^{chem} value (using Levine's (1971) expression for the solvation term and his suggested value of 30 for ϵ_{int}) such that the total absolute differences in predicted percent adsorption would be minimized. The value for ΔG_{Pb}^{chem} obtained in this manner was −9.46 Kcal/mol, which gave an average difference between theory and experiment of 15.5 percent adsorption, as shown by figure 12.

Table 5. Adsorption of lead from 50 milliliters solution onto 0.146 gram of adsorbent as function of pH and total lead content

ΣPb, *total lead, (moles per liter)*	pH *at 48 hours*	Pb *(milligrams per liter)*	Na *(milligrams per liter)*[1]	*Percent* Pb *adsorbed*
1.0×10^{-4}	1.83	18.8	2.0	9.3
1.0×10^{-4}	2.86	14.0	1.6	32.4
1.0×10^{-4}	3.83	4.0	4.0	80.7
1.0×10^{-4}	4.47	3.0	13.5	85.5
1.0×10^{-4}	5.73	0.7	13.5	96.6
5.0×10^{-4}	1.85	97.0	1.5	6.4
5.0×10^{-4}	2.78	92.5	1.3	10.7
5.0×10^{-4}	3.90	76.5	4.5	26.2
5.0×10^{-4}	4.38	68.8	7.0	33.6
5.0×10^{-4}	6.00	3.7	24.6	96.4

[1]Sodium concentrations above 2.0 mg/L are due to sodium hydroxide added in order to adjust the pH.

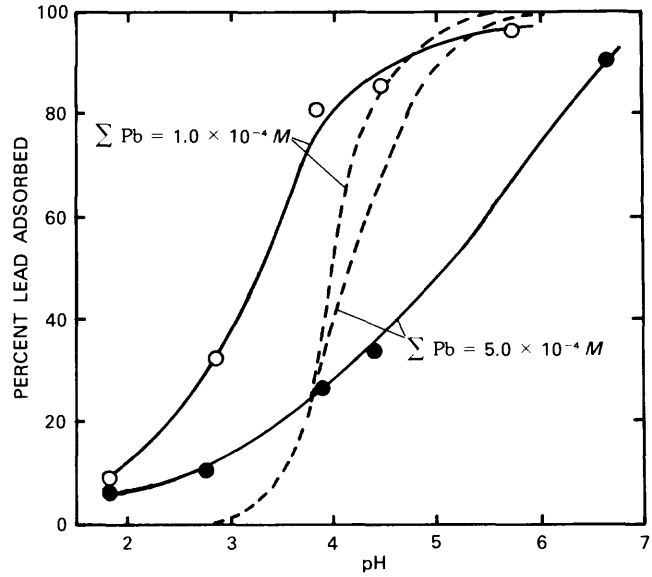

Figure 12. Adsorption of lead from 50-mL solutions onto 0.146-gram adsorbent for total lead concentrations of 1.0×10^{-4}(o) and 5.0×10^{-4} (•) molar, and comparison with best-fitting James-Healy predicted adsorption. (Solid lines outline experimental data; broken lines refer to predicted adsorption.)

Before going on to consider the predictive ability of the VSC−VSP model proposed by Bowden, Posner, and Quirk (1977), we might do well to resummarize the similarities and differences between this model and that of James and Healy (1972). First, both models use a Langmuir-type isotherm to describe the adsorption, with an equilibrium constant which can be defined for each chemical species by a free energy of adsorption consisting of terms which are independent of pH and ionic strength (such as ΔG_i^{solv} and ΔG_i^{chem} in the James-Healy model and a chemical "binding constant" K_i in the VSC−VSP model), and on a term which does depend on pH and ionic strength (such as ΔG_i^{coul} in the James-Healy model, and ψ_d in the VSC−VSP model).

The latter term's dependence on pH is the result of the pH-dependence of the electrical potential at the surface. The main difference between the two models exists in the manner in which the surface potential is calculated and in which it is said to change with distance from the surface (for example, linearly or in exponential decay) to the theoretical plane at which the ion is actually adsorbed.

As mentioned in an earlier section, the classical double-layer-model approach utilizes the assumption that the surface potential varies linearly in a Nernstian manner, decreasing 59 mV (at 25°C) per unit of pH increase, and equaling zero at the pH_{pzc}. Measurements of zeta potential (a physically measurable voltage which is closely related to the surface potential) by various in-

vestigators, however, have shown that such a dependence is not always obtained (R. O. James, oral commun., 1977) and that the surface potential often changes by substantially less than 59 mV per pH unit. The VSC–VSP model predicts a surface potential which is not only dependent on pH and ionic strength, but also on the total surface charge density of any adsorbed cations. As the adsorbed cation concentrations approach zero and the pH approaches the pH_{pzc}, however, the dependence of the surface potential on pH approaches the Nernstian ideal used by James and Healy (1972). The interrelationship of the various charge density and potential terms in the VSC–VSP model are illustrated by the method of calculating these quantities. Given a surface potential ψ_s and the potential-determining ion (H^+ and OH^-) activities, the surface charge density σ_s may be calculated from equation 42 based on the chemical and electrostatic interactions of the surface (as given by $K^{ads}_{H^+}$ and either $K^{ads}_{OH^-}$ or the pH_{pzc}) with these ions. From ψ_s and σ_s, the potential ψ_d is calculated by means of a rearranged equation 46. The diffuse layer charge density σ_d may then be calculated from ψ_d by use of equation 49. There, the value of σ_d is proportional to the square root of the ionic strength, which is a measure of the compression of the diffuse outer layer of charge near the surface. Finally, the value of ψ_d is used in equation 48 in order to determine the magnitude of the coulombic interaction of the surface with the adsorbed ions. When considered in conjunction with the pH-independent interactions accounted for in the solvation and "chemical" free energy terms, equilibrium considerations may then be used to calculate the surface concentrations Γ_i of the adsorbed species. These may then be substituted into equation 47 and its analogs in order to obtain the adsorbed cation charge density σ_i. Overall electroneutrality demands that the sum of the surface adsorbed, and diffuse charge densities that have been calculated (respectively, σ_s, σ_i, and σ_d) equal zero. If in such calculations they do not, then the value of the surface potential ψ_s, from which ψ_d, σ_s, σ_i, and σ_d were all derived, is adjusted accordingly, requiring a recalculation of all the other variables, so that the electroneutrality condition is satisfied. Such a procedure is easily adapted to an iterative computer program. Figure 13 shows calculation flow charts for both the VSC–VSP and the James and Healy (1972) models for heavy metals adsorption.

Like the model proposed by James and Healy (1972), the VSC–VSP model requires a comparison of experimental data and theoretical predictions in order to determine the magnitude of the chemical interactions (specifically the value of ΔG^{chem}_{Pb}), many component parts of which are fairly difficult to account for by theory. This VSC–VSP model, however, also unfortunately requires a knowledge of the "average" distance of approach d of an adsorbed cation to the surface. In reality, any model involving only one or two planes of adsorption near the surface will be an oversimplification of the true situation, particularly on surfaces as complex and irregular as oxides and impure silicates. Such a model is nevertheless used here because of its ability to

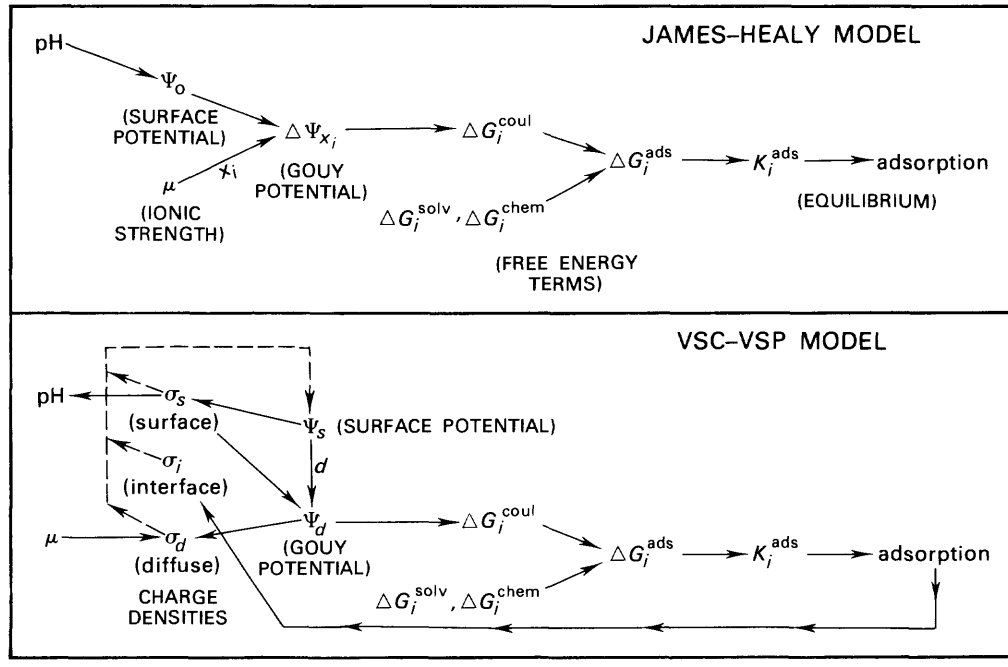

Figure 13. Flow charts for calculating adsorption in the James-Healy (1972) and VSC–VSP models.

describe adsorption phenomena approximately despite its simplicity. The concept of an "average" distance from the surface of an adsorbed cation does not arise from entirely theoretical considerations, and its usefulness lies in the fact that comparison of experimental data with theoretical predictions of adsorption for different values of d will yield a value which gives the best agreement. We might venture, however, that this "average" distance should lie somewhere between the crystal ionic radius (1.20 Å) of the Pb^{+2} ion and the radius of the ion with its first layer of attached water molecules or primary hydration sheath, as is normally used in the James-Healy model. (This latter value for both Pb^{+2} and $PbOH^{+}$ is 3.96 Å, which is the sum of the 1.20 Å ionic radius plus the 2.76 Å diameter of the water molecule.)

Just as the value of the "chemical" term of the free energy of adsorption was varied in the James-Healy model for the purpose of fitting as best we could the experimental data in table 5 to predicted values based on the pH and total lead content to give the agreement shown in figure 13, various values of d were used in a similar way in attempting to fit the VSC–VSP model to these data. (Indeed, Bowden, Posner, and Quirk (1977) used an approach of this sort to estimate the inner-layer capacitance, a measure of the value of d; they compared their experimental data, plotted as pH versus surface charge density, with a family of theoretical curves calculated using various capacitances, and selected the capacitance giving the best agreement with the experiment.) The values of the "chemical" free energy term and the "average" distance of approach of the adsorbed lead ions to the surface which would give the least disagreement between theory and experiment were found to be −12.28 Kcal/mol for ΔG^{chem}_{Pb} and 2.26 Å for d. The average deviation in percent adsorption between that found experimentally and that predicted using these values was a rather low 6.6 adsorption percent compared to the rather large 15.5 adsorption percent deviation obtained with the best fitting James-Healy model. The closer agreement of the VSC–VSP model is illustrated in figure 14, and a comparison of the predictive power of the two models is tabulated in table 6.

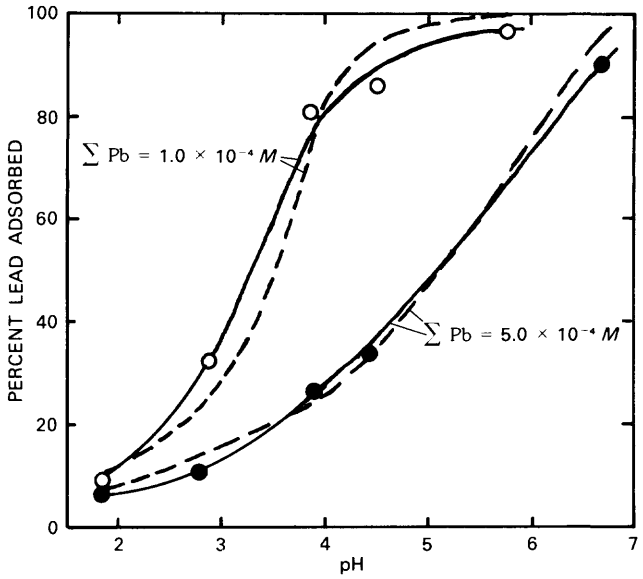

Figure 14. Adsorption of lead from 50-mL solutions onto 0.146 gram adsorbent for total lead concentrations of 1.0×10^{-4} (o) ad 5.0×10^{-4} (•) molar, and comparison with best-fitting VSC–VSP predicted adsorption. (Solid lines outline experimental data; broken lines refer to adsorption predicted.)

Table 6. Comparison of experimental and predicted adsorption of lead

Σ Pb, total lead (moles per liter)	pH	Percent adsorption of lead: Experimental	James-Healy model[1]	VSC–VSP model[2]
1.0×10^{-4}	1.83	9.3	0.048	9.34
1.0×10^{-4}	2.86	32.4	0.52	22.9
1.0×10^{-4}	3.83	80.7	24.6	70.8
1.0×10^{-4}	4.47	85.5	83.8	95.5
1.0×10^{-4}	5.73	96.6	99.9	99.9
5.0×10^{-4}	1.85	6.4	0.053	5.44
5.0×10^{-4}	2.78	10.7	0.43	10.8
5.0×10^{-4}	3.90	26.2	26.3	37.5
5.0×10^{-4}	4.38	33.6	65.7	53.0
5.0×10^{-4}	6.66	90.6	99.9	95.0

[1] $\Delta G^{chem}_{Pb^{+2}} = -9.46$ Kcal/mol and $x_i = 3.96$ A.

[2] $\Delta G^{chem}_{PbOH^{+}} = -12.28$ Kcal/mol and $d = 2.26$ A.

In incorporating Levine's (1971) expression for the solvation free energy term into the VSC–VSP model, we were faced with the dilemma of which value to use for the interfacial dielectric constant ϵ_{int}. Levine (1971) used a value of 30 in his solvation free energy term, while Bowden, Posner, and Quirk (1977) based their use of 6.0 for this term on work by Hasted, Ritson, and Collie (1948).

Instead of speaking of a dielectric constant which continuously varies with distance from the surface, however, we should rather speak of dielectric constants of each of the successive shells of adsorbed water molecules. The water shells very near the surface will have low dielectric constants due to the high electrical field and restriction of motion due to surface interactions, while the more distant shells will have higher dielectric constants. Bockris, Devanthan, and Muller (1963, p. 68) for this reason gave 6 as the dielectric constant value for the first layer of water molecules attached to the surface.

It, therefore, seems safe to say that as a first approximation, the interfacial dielectric constant within the first layer of adsorbed water molecules may be taken as the lower value of 6.0. It is the lower value of ϵ_{int} which we used in the Levine (1971) expression for the solvation free energy term, and in the ψ_d relation in the VSC–VSP model in order to obtain the predicted adsorption shown in figure 14 and tabulated in table 6. Our value of d of 2.26 Å lies well within the diameter (2.76 Å) of the first adsorbed layer of water so the approximation of a 6.0 dielectric constant should be valid. We should also note that this 2.26 Å value of d also lies comfortably within our earlier-suggested lower (1.20 Å) and upper (3.96 Å) limits for the parameter.

DISCUSSION AND CONCLUSION

The Effect of Cation Adsorption on Electrostatic Potential

A procedure for the characterization of a naturally-occuring silicate surface has been proposed by which one may predict the magnitude of adsorption of lead even when the adsorption sites may be nearly filled with cations other than those of lead, a situation one might expect to find in natural systems. While previous work has often been conducted under conditions where only trace quantities of lead or other heavy metal have been placed in contact with an adsorbent (in the absence of significant concentrations of adsorbing cations other than H^+), very few of these approaches have dealt with the problems faced when most of the adsorbent sites are occupied. The usefulness of the VSC–VSP model of Bowden, Posner, and Quirk (1977) in taking this into account is illustrated here by demonstration of the effect of adsorbed species on the electrostatic potential which, in turn, acts on the adsorbing ions.

The effect of increasing the concentration of cations other than lead on the electrostatic potential at distance d (where adsorption is presumed to take place), can be evaluated in part by substituting higher values of ionic strength in the calculation cycle. The solute postulated for this purpose is a uni-univalent salt that does not otherwise interact with lead.

When a given number of equivalents of adsorbent is placed in contact with a comparatively large number of moles of cations, some of which will attach to the adsorbent, any quantity of cations which is adsorbed will oppose further adsorption in two ways. First, of course, the process of adsorption will reduce the number of sites (and also the amount of cations) available for further adsorption. Second, and more important, however, is that further adsorption will be additionally opposed because the surface potential ψ_s will become more positive. Since the surface charge density σ_s decreases as the potential ψ_s increases (due to the $-K_{OH^-}[OH^-]e^{+F\psi_s/RT}$ term in equation 42), the former will become less positive (or more negative, as the case may be) in order that electroneutrality will be preserved.

Figure 15 shows how the total lead concentration ΣPb affects the surface potential in adsorbent slurries of the type for which data was earlier shown in table 5. Increased cation adsorption will also affect the electrostatic potential ψ_d at the "average" plane of adsorption of the cations. Since this electrostatic potential decreases from the surface potential in linear proportion to the surface charge density σ_s(see eq 46), and since increased cation adsorption works to make σ_s more negative, the potential ψ_d at the plane of cation adsorption should become more positive (or less negative) so that the tendency will be to restrict future cation adsorption. This effect is shown in figure 16 also for adsorbent slurries of the type analyzed earlier, and the effect causes the potential at the adsorption plane to differ greatly from that predicted by classical double-layer theory and is shown in figure 17 for comparison. It can be seen from figure 17 that a total lead concentration of 5.0×10^{-4} *M* (which is of the same general magnitude as the CEC of 1.0×10^{-3} eq/L) has a profound effect on ψ_d, making it positive even at values of pH above the pH_{pzc} and becoming more positive as pH increases. The result

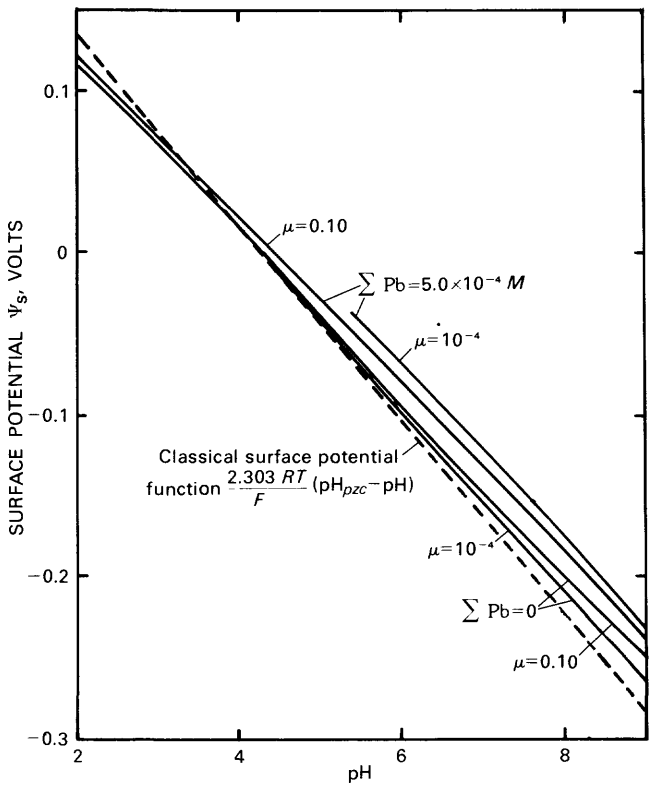

Figure 15. Effects of pH, ionic strength, and total lead on adsorbent's VSC–VSP surface potential.

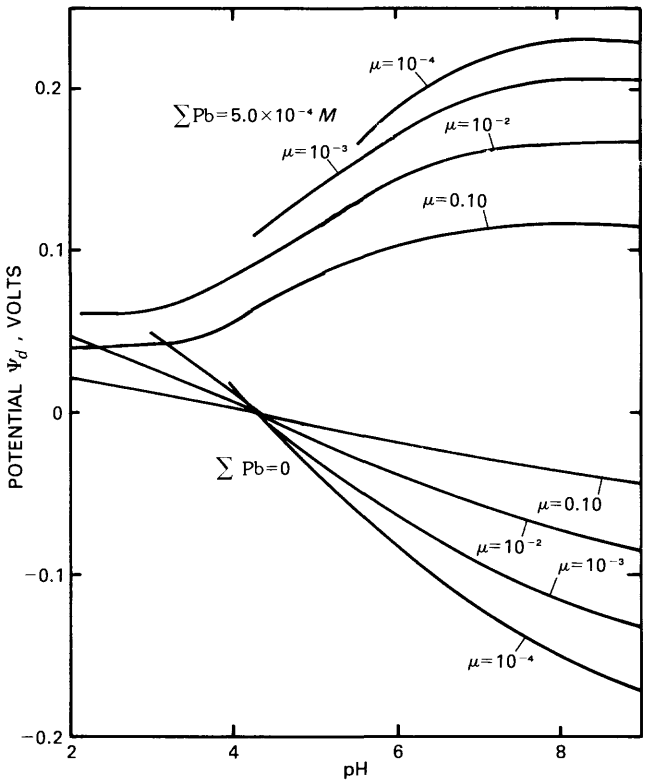

Figure 16. Effects of pH, ionic strength, and total lead on adsorbent's VSC–VSP electrostatic potential at the 2.17-Å adsorption plane.

is a potential which actually tends to desorb rather than adsorb cations. (Cations may still adsorb as the result of the opposing and perhaps overriding chemical interactions to which the free energy term ΔG_{Pb}^{chem} refers, however.) As for the fact that this tendency to hinder further cation adsorption appears to increase with pH, one might then wonder why lead adsorption nevertheless continues to increase as the pH increases. It would seem that if the tendency to desorb cations (a positive surface potential) became greater with pH, as is indicated by the rising potential for the $5.0\times10^{-4}M$ set of curves in figure 16, lead adsorption should perhaps decrease with pH. We must remember, however, that it is the increase in the adsorption itself which results in the unusual rise in electrostatic potential with pH. The overall effect of a rise in pH is not to cause desorption, but to prevent adsorption from increasing as quickly with pH as it would otherwise do in the absence of this effect.

An increase in pH will also result in an increase in the aqueous activity of $PbOH^+$ at the expense of Pb^{+2}. If $PbOH^+$ were the predominantly adsorbing species, then an increase in its aqueous activity relative to that of Pb^{+2} as a result of pH increase would cause further adsorption despite the opposing effect of a more positive ψ_d. We concluded in an earlier section from the decrease in pH accompanying lead adsorption that some univalent adsorption of $PbOH^+$ was indeed occurring, perhaps accompanied also by Pb^{+2} adsorption at lower values of pH.

The VSC–VSP model, as applied to the conditions of, and the material used in our experiments, does indeed predict that $PbOH^+$ will be the predominantly adsorbing species of lead above pH 4, as in shown in figure 18. Here we have defined a "mean adsorption valence" which is simply the average number of moles of sites used for adsorbing a mole of lead. A value of 2 indicates Pb^{+2} is the only form adsorbed and a value of 1 indicates $PbOH^+$ is the only form adsorbed. It appears from the theoretically calculated example of figure 18 that $PbOH^+$ is the predominantly adsorbed species within the pH range encountered in most natural waters. The contribution of Pb^{+2} adsorption should not always be considered negligible under all circumstances, however.

Natural waters will certainly not contain total lead or other heavy metal concentrations as large as the $5.0\times10^{-4}M$ value used here. Sediments in contact with natural waters, however, will undoubtedly have a large fraction of their adsorption sites occupied with major cations, such as Ca^{+2}, Mg^{+2}, K^+, or Na^+. The presence of cations such as these near the plane at which heavy metal

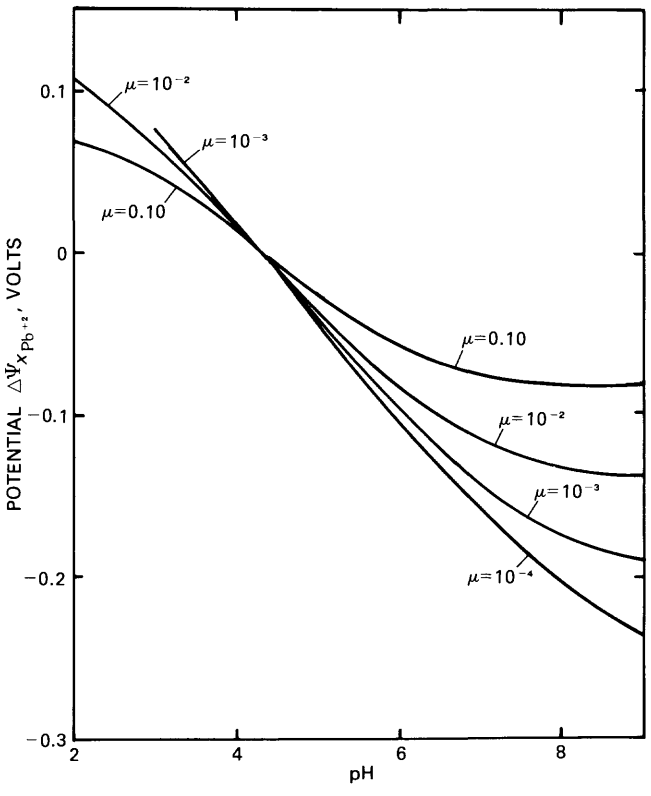

Figure 17. Effects of pH and ionic strength on adsorbent's James-Healy electrostatic potential at the 3.96-Å adsorption plane.

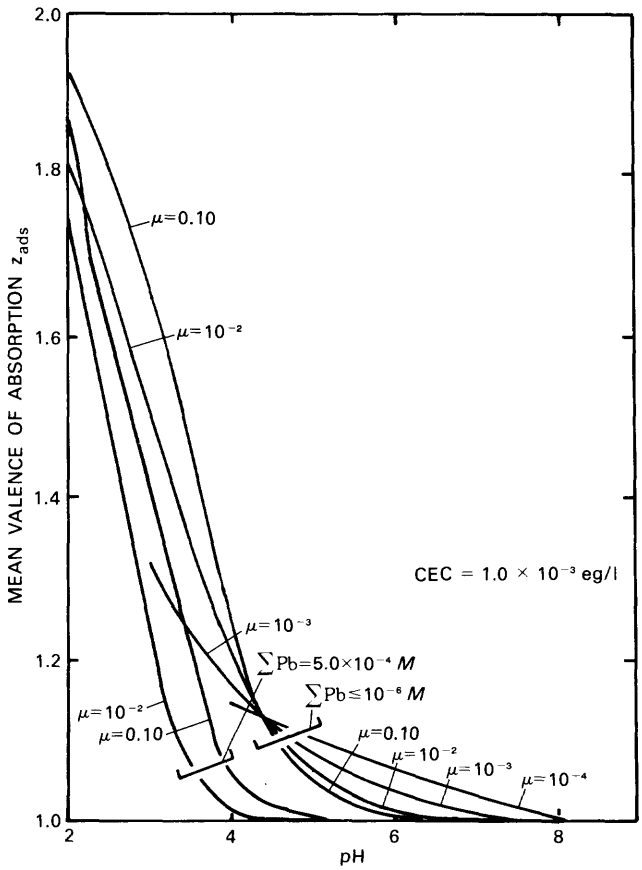

Figure 18. Effects of pH, ionic strength, and total lead on mean valence of adsorption of lead on adsorbent, as per the VSC–VSP model.

cations adsorb will, according to the VSC–VSP model, have somewhat the same effect in opposing a further cation adsorption as did the large surface concentrations of adsorbed lead in our experiments. It would, therefore, seem that if we are to aim toward eventual prediction of heavy metal adsorption in the presence of the other major and minor solute species normally encountered in natural waters, the use of the VSC–VSP model will be necessary in order to assist us in more precisely accounting for the interactions among the various adsorbed and dissolved species. The model obviously has much greater flexibility than simple mass-law or adsorption isotherm models.

The Effect of Varying Total Lead Content

It has recently been shown by M. M. Benjamin (unpub. data, 1977) that the position of the adsorption edge, that is, the steepest rise with pH of the percent of the metal adsorbed is affected by total heavy metal concentration to a much greater degree than would be predicted by classical double-layer models of adsorption.

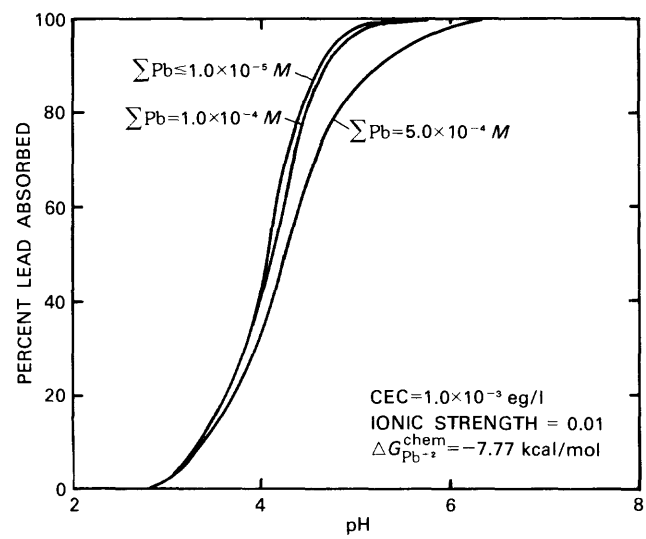

Figure 19. Effect of total lead concentration on pH-dependent adsorption at 0.010 *M* ionic strength according to James-Healy model.

Figure 19 shows the pH-dependence of lead adsorption which would be predicted using the chemical free-energy value that was used to fit the James-Healy model to the data in table 5. It can be seen that the rises in adsorption with increasing pH, predicted by the James-Healy model, are rather similar for total lead concentrations which differ by an order of magnitude or more. Only when the total lead concentration ΣPb at $5.0\times10^{-4}M$ closely approaches the CEC of 1.0×10^{-3} eq/L does it become slightly more difficult to effect increased adsorption by increasing the pH. Figure 20, however, shows the much

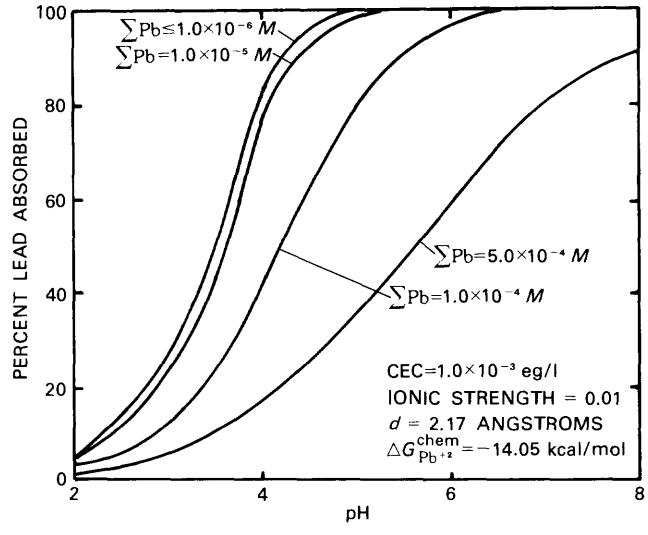

Figure 20. Effects of total lead concentration on pH-dependent adsorption at 0.010 *M* ionic strength, according to VSC–VSP model.

larger effect of total lead concentration on the pH-dependence predicted by the VSC–VSP model. It can be seen that the predicted shift in the adsorption edge is much larger, in some cases exceeding one pH unit, as compared to a few tenths of a pH unit maximum shift predicted by the James-Healy model. This illustrates the effect of the adsorbed lead cations in making the adsorption potential ψ_d more positive and thereby opposing further adsorption at higher surface concentrations. The fact that the VSC–VSP model predicts an observed effect which cannot be accounted for on the basis of classical double-layer theory lends support to its use in modeling heavy metal adsorption.

REFERENCES CITED

Armistead, C. G., Tyler, A. J., Hambleton, F. H., Mitchell, S. A., and Hockey, J. A., 1969, The surface hydroxylation of silica: Journal of Physical Chemistry, v. 73, no. 11, p. 3947–3953.

Atkinson, R. J., Posner, A. M., and Quirk, J. P., 1967, Adsorption of potential-determining ions at the ferric oxide–aqueous interface: Journal of Physical Chemistry, v. 71, no. 3, p. 550–558.

Baes, C. F., Jr., and Mesmer, R. E., 1976, The hydrolysis of cations: New York, Wiley, p. 358–365.

Bilinski, Halka, and Stumm, Werner, 1973, Pb(II) species in natural waters: Swiss Federal Institute of Technol. EAWAG News no. 1, Jan. 1973.

Bockris, J. O'M., Devanthan, M. A. V., and Muller, K., 1963, On the structure of charged interfaces: Proceedings of the Royal Society Series A, v. 274, p. 55–79.

Bowden, J. W., Posner, A. M., and Quirk, J. P., 1977, Ionic adsorption on variable charge mineral surfaces. Theoretical-charge development and titration curves: Australian Journal of Soil Science, v. 15, p. 121–136.

Chapman, H. D., 1965, Cation exchange capacity, *in* C. A. Black, ed., Methods of soil analysis, Agronomy Series no. 9, Madison, Wisconsin: American Society of Agronomy, Inc., part 2, p. 891–901.

Davis, J. A., James, R. O., and Leckie, J. O., 1978, Surface ionization and complexation at the oxide/water interface: Journal of Coloid and Interface Science, v. 63, no. 3, p. 480–499.

Garrels, R. M., and Christ, C. L., 1964, Solutions, minerals, and equilibria: New York, Harper and Row, 450 p.

Hasted, J. B., Ritson, D. M., and Collie, C. H., 1948, Dielectric properties of aqueous ionic solutions, Parts I and II: Journal of Chemical Physics, v. 16. no. 1, p. 1–21.

Hem, J. D., 1976, Geochemical controls on lead concentrations in stream water and sediments: Geochimica et Cosmochimica Acta, v. 40, p. 599–609.

Hem, J. D., and Durum, W. H., 1973, Solubility and occurrence of lead in surface water: Journal of the American Water Works Association, v. 65, no. 8, p. 562–568.

James, R. O., and Healy, T. W., 1972, Adsorption of hydrolyzable metal ions at the oxide-water interface III. A thermodynamic model of adsorption: Journal of Colloid and Interface Science, v. 40, no. 1, p.65–81.

James, R. O., and Parks, G. A., 1982, Characterization of aqueous colloids by their electrical double layer and intrinsic surface chemical properties, *in* Egon Matejevic, ed., Surface and Colloid Science, v. 12, New York, John Wiley, p. 119–216.

Krishnamoorthy, C., and Overstreet, Roy, 1949, Theory of ion-exchange relationships: Soil Science, v. 68, p. 307–315.

Lal, K., and Parshad, R., 1974, Test and utilization of the Fricke and Pearce equations for dielectric correlation between powder and bulk: Journal of Physics D, Applied Physics, v. 7, no. 3, p. 455–461.

Lawrie, D. C., 1961, A rapid method for the determination of approximate surface areas of clays: Soil Science, v. 92, p. 188–191.

Levine, Samuel, 1971, Remarks *on* Discreteness of charge and solvation effects in cation adsorption at the oxide/water interface by G. R. Wiese, R. O., James, and T. W. Healy, (*in* Discussions of the Faraday Society, v. 52, p. 302–311): Discussions of the Faraday Society, v. 52, p. 41A–42A.

Lind, C. J., 1978, Polarographic determination of lead hydroxide formation constants at low ionic strength: Environmental Science and Technology, v. 12, p. 1406–1410.

Looyenga, H., 1965, Dielectric constants of heterogeneous mixtures: Physica, v. 31, p. 401–406.

Nriagu, J. O., 1974, Lead orthophosphate-IV. Formation in the environment: Geochimica et Cosmoshimica Acta, v. 38, p. 887–898.

Schindler, P. W., Furst, B., Dick, R., and Wolf, P. U., 1976, Ligand properties of surface silanol groups: Journal of Colloid and Interface Science, v. 55, no. 2, p. 469–475.

Stumm, Werner, and Morgan, J. J., 1970, Aquatic Chemistry: New York, Wiley Interscience, 583 p.

Truesdell, A. H., and Christ, C. L., 1968, Cation exchange in clays interpreted by regular solution theory: American Journal of Science, v. 266, p. 402–412.

U.S. Geological Survey, 1974, Quality of surface waters of the United States; 1970, pt. 11, Pacific slope basins in California: U.S. Geological Survey Water-Supply Paper 2159, p. 118–120.

———1976, Surface water supply of the U.S. 1966–1970, pt. 11, v. 2: U.S. Geological Survey Water-Supply Paper 2129, 194 p.

Vanselow, A. P., 1932, Equilibria of the base-exchange reaction of bentonites, permutites, soil colloids, and zeolites: Soil Science, v. 33, p. 95–113.

Wiese, G. R., James, R. O., and Healy, T. W., 1971, Remarks *on* Discreteness of charge and solvation effects in cation adsorption at the oxide/water interface by G. R. Wiese, R. O. James, and T. W. Healy, (*in* Discussions of the Faraday Society, v. 52, p. 302–311): Discussions of the Faraday Society, v. 52, p. 41A–42A.

Yadav, A. S., and Parshad, R., 1972, A formula for dielectric correlation between powder and bulk over wide ranges of permittivities and packing fractions: Journal of Physics D, Applied Physics, v. 5, p. 1469–1463.

U.S. GOVERNMENT PRINTING OFFICE: 1984—777-085